CERN LAB II/BT/Int./72-5

EUROPEAN ORGANIZATION FOR NUCLEAR RESEARCH

BEAM DUMPING IN THE SPS

P. Faugeras, W.C. Middelkoop, B. de Raad, G. Schröder and P. Sievers

ABSTRACT

Uncontrolled beam loss in the SPS will cause thermal and radiation damages of machine components as well as induced radioactivity. An internal beam dumping system is needed to prevent such an uncontrolled beam loss. Variants of two possible dumping methods have been studied and compared on technical feasibility, dumping efficiency and cost. One method uses fast kicker magnets to dump the beam in one SPS revolution by a constant displacement onto an absorber block. The other is based on a growing closed orbit bump which displaces the beam over several revolutions onto the block with a defined rate of displacement per revolution. The technical problems of the absorber block are raised.

Geneva - 9th October, 1972

EUROPEAN ORGANIZATION FOR NUCLEAR RESEARCH

LAB II/BT/Int/72-5

BEAM DUMPING IN THE SPS

by

P. Faugeras, W.C. Middelkoop, B. de Raad, G. Schröder and P. Sievers

Geneva - 9th October, 1972

TABLE OF CONTENTS

Page

APPENDICES

1. Introduction

During some of the acceleration time the accelerated beam will not be used for physics experiments. This will occur during the running-in period, during machine development shifts and during the setting-up of slow and fast extractions. In the latter case the external beam will be dumped onto an absorber block at the beginning of each beam transfer line.

The kinetic energy of a beam of 10^{13} p/p at 400 GeV/c amounts to 640 kJ. This would be sufficient for melting 0.7 kg of steel if the lost energy would not be spread out due to the spatial development of the nuclear shower. It remains, however, that the repeated loss of beam pulses at the same point of the main ring amounts to a continuous local dissipation of 100 to 160 kW, depending on the cycle and the beam momentum. Severe thermal damage of main ring equipment would be the result if no internal beam dumping system would be available to prevent such an uncontrolled beam loss.

The other reason for having an internal beam dumping system is the need to reduce as much as possible both the radiation damage of machine components and the induced radioactivity which results from uncontrolled beam loss.

Estimates of the temperature rise show that at the maximum beam intensity, even the loss of a single beam pulse at one spot will probably cause thermal damage of the vacuum chamber. Therefore the beam dumping system should be designed such that it can, after the addition of a suitable control system, serve as an emergency dumping system whenever the uncontrolled beam loss tends to approach the permissible limit.

2. Possible Beam Dumping Schemes and General Assumptions

2.1 Dumping Schemes

In order to satisfy the requirements defined in chapter 1, it is necessary to dump the beam in a fast and clean way by displacing it onto the front surface of an absorber block by means of a pulsed magnet system. The dimensions of the absorber block must be sufficiently large to contain practically the entire nuclear shower produced during dumping and to provide sufficient self-shielding against the induced radioactivity in the centre of the block. The block must therefore have a hole in its centre through which the circulating beam can pass. It is proposed to place the dumping system in the long straight section LSS 4 of the SPS.

There exist two possible methods for a fast displacement of the beam onto the front surface of the block. One method uses fast kicker magnets to dump the beam in one revolution by a constant beam displacement. The other is based on a growing closed orbit bump with its maximum amplitude at the front surface of the absorber block. This bump displaces the beam over several revolutions onto the block with a defined rate of displacement per revolution. Both methods must be able to dump the full aperture of the SPS at all momenta up to 400 GeV/c in order to cope without restrictions with all conditions that may require internal beam dumping. Moreover, the methods must be compatible with any reasonable choice of Q-values for the SPS.

A one turn beam dumping system requires fast kicker magnets each being excited by a rectangular current pulse of about 23 μsec length. Each current pulse is generated by the discharge of a pulse forming network (pfn) through the magnet into a matched terminating resistor. The main parameters of such a system are the total beam displacement at the front surface of the absorber block, which determines the bending strength of the magnets, and the risetime of the kick strength which determines the proton loss elsewhere around the SPS. This risetime must therefore be short compared with the revolution time.

A detailed treatment of beam dumping with fast kicker magnets within half a lattice period as well as over a full period is given in chapter 3. Dumping within half a period requires that the kicker magnets are placed adjacent to a quadrupole with the absorber block upstream of the next quadrupole. In case of dumping over a full period, the deflected beam has to pass through a quadrupole between the kicker magnets and the dump block which imposes limitations on the beam excursion within its aperture. This requires an additional absorber block in front of the intermediate quadrupole in order to protect the latter from being irradiated.

The method of beam dumping with a growing closed orbit (c.o.) bump is treated in detail in chapter 4. For Q = 27.75 the phase advance over one long straight section is 185°. Therefore, it is just possible to produce a half wavelength bump with magnets adjacent to the two outer QF's. The magnets can be excited with half sine wave current pulses by discharging a capacitor into the inductance of each magnet. The synchronous excitation of the two magnets produces a closed orbit bump of growing amplitude which drives the beam onto the front surface of the absorber block placed at the crest of the bump just in front of the central QF in LSS 4. The rate of displacement depends on the period of the sine wave and can conveniently be chosen around 10 mm/revolution.

The beam excursion is limited by the aperture of the intermediate QD between the first bumper magnet and the absorber block. In an endeavour to avoid this limitation, we have also studied a more complicated system which requires four bumper magnets and which bumps the beam over one instead of two periods.

Some aspects of the beam dump absorber block will be described in chapter 5. For the moment, we merely remark that beam dumping by fast kickers gives a constant beam displacement which displaces the whole beam onto the front surface of the dump some millimetres away from the dump edge. The only beam loss outside the block is due to the protons which during the rise time are not sufficiently displaced to be dumped on the

dump block and which are lost elsewhere around the aperture of the SPS.

Beam dumping with a bump of growing amplitue displaces the beam also onto the front of the dump, but with the maximum of the proton intensity at the edge of the aperture of the block which reduces the efficiency of the latter.

The conclusions of the different methods of dumping considered will be drawn in chapter 6.

2.2 General Assumptions

The apertures of the magnets and the dump block are calculated for the assumptions that the horizontal half aperture A_x = 76 mm at $(\beta_H)max$ = 109.2 m and $(\alpha_p)max$ = 4.25 m and for a momentum spread of $\Delta p/p$ = 2 °/oo. The half aperture required for dispersion at $(\alpha_p)max$ is therefore 8.5 mm and the resulting half horizontal aperture for c.o. deviations and beam size is 67.5 mm.

The vertical half aperture is limited to 24.25 mm by the vacuum chamber at the upstream side of the B2 magnets where β_V = 103.1 m . The maximum vertical aperture at $(\beta_V)max$ = 109.2 m is therefore A_z = 24.95 mm.

The required half apertures at any point around the accelerator can therefore be calculated with

$$A_x = (76-8.5)\left(\frac{\beta_H}{109.2}\right)^{\frac{1}{2}} + 2.10^{-3}\,\alpha_p$$

and

$$A_z = 24.25\left(\frac{\beta_V}{103.2}\right)^{\frac{1}{2}}$$

The aperture of the magnets is calculated for the maximum β-values along their length. In addition, we have allowed for the beam displacement due to deflection, and for a clearance of about 1.5 mm all around the aperture. It has further been assumed that the pulsed magnets are mounted

in vacuum tanks, and therefore no allowance is made for a vacuum chamber in the magnet gap.

The deflection is determined by the required beam displacement at the upstream side of the dump block. Depending on whether the beam is dumped horizontally or vertically and on whether the dump block is placed in front of a QF or a QD, the required nominal aperture for the hole of the dump block may be larger at its downstream end rather than at its upstream side. In these cases, the required beam displacement at the dump block is minimized by aligning the side, where the beam is dumped, parallel to the envelop of the nominal machine aperture. The dump block will have a length of 4 m and the distance between the end of the dump to the yoke of the adjacent quadrupole is 1.3 m. This distance is determined by the space requirements for a correcting dipole and a pick-up station.

3. Beam Dumping with Fast Kickers

Single turn ferrite magnets must be used for the deflection of the beam, due to the required fast rising current pulses. Their maximum field is limited to about 0.35 T, due to the saturation of the ferrite.

The inductance of each magnet of length ℓ, gap width w and gap height h is

$$L = \mu_o * \frac{w}{h} * \ell .$$

The required current is

$$I = \frac{B * h}{\mu_o} .$$

The charging voltage on the pfn of characteristic impedance Z becomes

$$U = 2Z * I$$

and the time constant of the exponentially rising current pulse is

$$\tau = \frac{L}{2Z} .$$

In our case the impedance must be chosen as low as possible in order to limit the charging voltage of the pfn to less than about 60 kV. A practical lower limit is given by the number of parallel coaxial high voltage cables between each pfn and magnet which is still reasonable and by the permissible risetime of each magnet module. For the following calculations, we shall assume that the pfn has a characteristic impedance $Z = 3\Omega$.

3.1 Kicking within Half a Lattice Period

We assume that the deflection system consists of 4 ferrite magnets of equal dimensions, each being excited by its own pulse forming network.

In case of horizontal dumping the current for a magnet placed near a QF is smaller than the current of a magnet placed near a QD, because of the aspect ratio w/h and of different deflections for both cases. The inverse is valid for vertical dumping.

We assume that the magnets are placed downstream of QF 4181 for horizontal and downstream of QD 4171 for vertical dumping. Each magnet is 4 m long. The distance between two adjacent magnets is 0.3 m. The distance between the downstream side of the quadrupole and the upstream side of the adjacent kicker magnet is 0.8 m. The geometrical layout is given in Fig.3.1. Both dumping systems must displace the beam over the full aperture of the absorber block plus at least one additional millimeter in order not to dump the protons too near to the edge of the absorber block. This leads to the following magnet characteristics :

Table 3.1

		Horizontal	Vertical
Machine aperture at the upstream side of the absorber block	(mm)	67.5	24.5
Beam displacement in front of absorber block	(mm)	68.5	25.5
Deflection angle	(mrad)	4.77	1.78
Total kick strength $\int Bd\ell$ at 400 GeV	(Tm)	6.4	2.37
Magnetic field	(T)	0.4	0.148
Magnet length	(m)	4.0	4.0
Magnet gap width w	(mm)	166.	57.5
Magnet gap height h	(mm)	39.0	103.0
Current	(kA)	12.3	12.1
Inductance per magnet	(μH)	21.4	2.81
Time constant (τ)	(μs)	3.56	0.467
Charging voltage of the pfn	(kV)	74.0	72.8

The maximum permissible current for thyratrons is about 10 kA for a pulse length of 24 μs. * However, this has to be confirmed by prototype tests. Therefore, in spite of the choice of very long magnets, the currents and voltages required are nevertheless too high for both systems. In addition, the risetime ($T_R \approx 3\tau$) is much too long for horizontal dumping, whereas it is marginal for vertical dumping. The horizontal dumping system is therefore unsuitable for our requirements. Moreover, the high cost (Appendix I) is an additional drawback for both dumping systems.

3.2 Kicking over One Lattice Period

We will now study for horizontal deflection a layout as shown in fig. 3.2 in which the magnets are placed downstream of QF 4161 and the absorber block upstream of QF 4181. For vertical deflection, the magnets are placed downstream of QD 4171 and the absorber block upstream of QD 4191.

3.2.1 Main Parameters

We assume that the deflection system consists of 2 magnets of equal dimensions, each having its own pulse generator. The length of each magnet is 2.5 m and the distance between the two magnets 0.3 m. The distance between the downstream side of the quadrupole and the upstream side of the kicker magnet is 0.8 m.

This leads to the characteristics of the system as given in Table 3.2.

---

* H. Menown, English Electric Valve Co., Private Communication

Table 3.2

		Horizontal	Vertical
Machine aperture at the upstream side of the absorber block	(mm)	118	43
Beam displacement in front of absorber block	(mm)	119	44
Deflection angle	(mrad)	1.4	0.52
Total kick strength $\int Bd\ell$ at 400 GeV	(Tm)	1.85	0.69
Magnetic field	(T)	0.37	0.14
Magnet length	(m)	2.5	2.5
Magnet gap width w	(mm)	133	51
Magnet gap height h	(mm)	27.5	72
Current	(kA)	8.1	7.9
Inductance per magnet	(μH)	15.19	2.2
Time constant (τ)	(μs)	2.53	0.37
Charging voltage of the pfn	(kV)	48.5	47.6

In view of the current requirements, both systems can possibly be built. However, the risetime ($T_R \simeq 3\tau$) of the horizontal system is far too long. On the other hand, the expected risetime of the vertical system leads to acceptable beam losses, as will be shown in chapter 3.3. It is therefore assumed that this latter system is adopted for the remaining part of chapter 3.

3.2.2 Aperture and Shielding Requirements for QF 4181

The deflected beam has to pass through the aperture of QF 4181. The maximum possible beam excursion in this aperture without touching the vacuum chamber is sketched in fig. 3.3 for the nominal beam size at injection. Table 3.3a summarises the maximum possible beam excursions for several beam sizes and horizontal closed orbit deviations.

For the purpose of this table we have made the unrealistic assumption that one would know exactly the beam size at the moment of dumping

and that the kick strength is adjusted such that the kicked beam has just 1 mm clearance with respect to the vacuum chamber in QF 4181. Table 3.3a also indicates the percentage of the vertical beam size which falls on the absorber for the maximum permissible deflection as defined in the previous sentence. In the calculation of this maximum permissible deflection, the vertical c.o. deviation has only to be taken into account if its phase is different from the phase of the kick. In the most pessimistic case, protons can have a certain positive c.o. deviation in QF 4181 and a corresponding negative c.o. deviation at the front of the absorber block. The allowance required in QF 4181 is then 1.3 mm, for a vertical closed orbit deviation of 5 mm at (β_V) max, as calculated in Appendix IIIa.

Table 3.3

a_x at (β_H)max and $\alpha_p = 0$	COH at (β_H)max	a_z at (β_V)max	possible deflection at the downstream side of QF 4181	percentage of vertical beam size falling onto the absorber block
mm	mm	mm	mm	
a) normal quadrupole				
27.6	10	10.0	11.0	100
27.6	0	19.25	8.2	54.3
27.6	10	19.25	7.2	45.9
57.5	0	19.9	4.2	25.7
57.5	10	19.9	2.2	5.4
b) enlarged quadrupole				
27.6	10	19.25	18.7	100
50.0	0	19.9	13.8	100
57.5	10	19.9	10.9	76

In table 3.3, the normalized betatron amplitudes a_x = 27.6 mm and a_z = 19.25 mm correspond to the nominal beam emittances at injection at 10 GeV/c *. The values a_x = 57.5 mm and a_z = 19.9 mm correspond to a beam which just fills the available SPS aperture, taking into account a c.o. deviation of horizontally 10 mm and vertically 5 mm.

Table 3.3a shows that the deflection allowed for large beams is not sufficient to place the beam onto the absorber block. Only a beam with a vertical half size of $a_z \leq 10$ mm at (β_V)max can pass through QF 4181 without touching its vacuum chamber and be fully dumped on the absorber block.

One might think that this problem can readily be cured by shielding QF 4181 by an additional absorber block in front of QF 4181. This block would have an aperture and a layout as defined in chapter 2.2. Deflected protons which are outside the aperture of QF 4181 would be dumped on this block (called absorber 1 in the following), whereas protons with less deflection would be dumped on the main block half a lattice period downstream (absorber 2). However, due to the vertical betatron phase shift of 23.4° between the front of absorber 1 and the downstream side of QF 4181, this quadrupole cannot be shielded completely by absorber 1, even if the vertical aperture of the latter is equal to the nominal machine aperture (see Appendix IIIb). The normal QF 4181 can be completely protected only if absorber 1 reduces the vertical aperture by a factor of 0.5 to 0.75, depending on the detailed assumptions on beam sizes and c.o. deviations, which is clearly not acceptable.

In order to assess the effects of the partial shielding of the vacuum chamber of the normal QF 4181 by absorber 1, we have considered what will happen in two very different cases, namely a beam which is blown up to the full size of the vacuum chamber and a beam with the nominal design dimensions at 400 GeV/c.

---

* The 300 GeV programme, CERN 1050.

For the full aperture beam we have taken half sizes $\hat{a}_x$ = 57.5 mm and $\hat{a}_z$ = 19.9 mm. The vertical displacement at the front of absorber block 2 was taken equal to the local vertical machine aperture plus 1 mm, i.e. 44 mm. The proton density in phase space was assumed to be constant. The calculated percentages of protons lost on the vacuum chamber of QF 4181 are 5.2 % for a standard vacuum chamber and 2.5 % for a specially shaped vacuum chamber which has the same width, but follows the pole profile of a normal quadrupole.

These figures are several times larger than the calculated inefficiency of the beam dumping system. However, they would not affect the quadrupole vacuum chamber although they do increase the radiation damage to the quadrupole. On the other hand, the effect of an incomplete shielding of the normal QF 4181 by the absorber block 1 is dangerous in case of a high energy beam of design emittance. There are situations where such a small beam can pass through absorber 1 and hits the vacuum chamber of QF 4181, instead of being dumped on absorber 2.

The aperture limitation given by absorber 1 at the downstream side of QF 4181 is shown in fig. 3.4 for the design beam at 400 GeV/c. In other words, any proton whose vertical position is above this limit at the downstream side of QF 4181, would have been intercepted by absorber 1. This means that if one wants to avoid the beam hitting the normal vacuum chamber, the horizontal position of the centre of the beam must stay in the interval $\pm$ 19.0 mm, during the vertical dumping process.

The situation could be improved by a special vacuum chamber. The horizontal half width of the vacuum chamber could be limited to 68.3 mm, instead of 76 mm, due to the fact that $\alpha_p \simeq 0$ in the long straight section. Then one gains a few millimetres in the chamber height, and the horizontal maximum excursion for the centre of a small beam is now $\pm$ 35 mm. However, as will be shown below, a restriction of the horizontal aperture at QF 4181 is undesirable in view of the radial beam displacement required during the scraping of the halo of the beam.

Under the assumption that the radius of the inscribed circle of QF 4181 is enlarged by a factor 11/9, as for the enlarged quadrupoles foreseen for slow extraction, larger beams can pass through the aperture of such a quadrupole and be properly dumped (Table 3.3b). A beam of nominal size at injection can now pass the enlarged QF 4181 and be fully dumped onto the absorber block.

Moreover, it is then possible to dump any beam without loss in such an enlarged quadrupole unless the horizontal half beam size is larger than 50 mm (Table 3.3b). A beam loss of 2 % on the quadrupole would occur for the extreme case of a beam which is accidentally blown up to a maximum half horizontal beam size of 57.5 mm, but this would be acceptable. One could therefore consider not to protect the enlarged QF 4181 with the additional absorber block 1. This block is,however, necessary as a protection in case of faulty tracking of the voltage on the pulse generator and for the disposal of beams of less than 40 GeV/c. This latter condition is due to the limited range of voltage on the thyratrons, which do not fire properly if the applied voltage is too low.

It is shown in Appendix IIIb and in Fig. III.b2 that an enlarged QF can be completely shielded by absorber block 1 without limiting the machine aperture. But only a beam with $\hat{a}_z \leq 6.5$ mm at (β_V)max and appropriate deflection can now pass through absorber 1 and be fully dumped on absorber 2. For $\hat{a}_z > 6.5$ mm the protons are shared between the two absorber blocks or can be deflected entirely onto the first block for sufficiently low beam momenta.

In case of a beam of design emittance at 400 GeV/c, an enlarged quadrupole with the suitably shaped vacuum chamber allows an horizontal maximum excursion for the beam centre of $\pm$ 65 mm, which is large enough to dump properly a small beam sitting anywhere in the machine aperture. (Fig. 3.4).

Such large horizontal beam excursions may occur during normal machine

operation, as shown by the following examples:

1) Scraping of the halo of the high energy beam is a normal operation during any cycle. For this process, the beam must be radially displaced toward the edge of absorber block 1 by means of slowly pulsed horizontal dipoles. The scraping efficiency depends strongly on the distance between the position of the scraper and the edge of the absorber block. We assume that this distance is 1 mm. If an emergency beam dumping is required during the scraping procedure, the beam at the downstream side of QF 4181 has a position as indicated in fig. 3.4.

2) There will be about 20 horizontal and vertical dipole magnets positioned around the machine for correcting the horizontal and vertical closed orbit, or to produce a c.o. bump for specific reasons like extraction and scraping. A faulty adjustment of any of these magnets may lead to a strongly deformed closed orbit at QF 4181. But it must be possible to dump the beam safely from the wide range of horizontal positions.

It is therefore necessary that QF 4181 is an enlarged quadrupole. For matching reasons, also QF 4161 must then be of the enlarged type.

3.3 System Efficiency

Three different fates can occur to the protons which are deflected during the risetime of the kick strength :

i) The deflection is so small that the protons stay in the machine aperture and are then dumped during the next revolution.

ii) The deflection is such that the betatron amplitude of the protons is larger than the available aperture, but not large enough to hit the absorber block. These protons are lost around the machine.

iii) The deflection is sufficiently large so that the protons are properly dumped during the first revolution.

We define the system efficiency as the ratio of the number of protons dumped on the absorber block to the total number of protons in the beam. The proton losses are proportional to the risetime and depend also on the beam size and the proton distribution in the beam as well as on the closed orbit deviation.

The following table 3.4 gives the system efficiency for a vertical kick over a whole lattice period for different half vertical beam sizes at (β_V)max and vertical closed orbit deviations. The time constant of the kicker magnets is 0.4 µs and the nominal displacement at the dump is 44 mm. All these calculations are made for a uniform proton distribution in the transverse phase plane, which represents the worst case.

Table 3.4

$\hat{a}_z$ mm at (β_V)max	$(c.o.v.)_{max}$ mm	system efficiency %
4.3	0	99.99
3.0	5	99.3
4.3	5	99.3
19.9	5	99.0
4.3	10	98.5

Whatever practical conditions are taken, the table shows that the system efficiency is better than 98.5 %.

4. Beam Dumping by a Closed Orbit Bump

4.1 General Remarks

For each of the schemes studied in this Chapter, we will compute the strengths of the bumper magnets, which are necessary to dump a beam of 400 GeV/c which may be anywhere in the aperture of the absorber block. Except in Chapter 4.4, we disregard the effects of the rate of beam displacement per revolution, of any change in the Q-value of the machine, and of a particular beam size.

In these schemes, the bumper magnets which create the closed orbit deformation, have pulse performance requirements which are much less stringent than those of a fast kicker system. Therefore, these magnets can have a laminated iron yoke, which means that the maximum magnetic field achievable in the magnet gap is at most 2 Tesla. Each magnet length is then chosen accordingly.

On the other hand, in view of the very high magnetic strengths required for all these schemes, as it will be seen below, the bumpers are assumed to be mounted in vacuum tanks. In addition to the problem of manufacturing an elliptically shaped ceramic vacuum chamber, a magnet with such a chamber in its gap would require about 50 % more energy than a magnet working under vacuum and giving the same deflection to the beam. The problems of electrical insulation and of mechanical stresses in the magnet coil remain about the same in both cases.

The inductance L of a particular bumper magnet of length ℓ, gap width w, gap height h, and with N turns, is given by :

$$L = N^2 * \mu_o * \frac{w}{h} * \ell \qquad (4.1)$$

The current I, necessary to get the required magnetic strength $B * \ell$ is:

$$I = \frac{B * h}{\mu_o} * \frac{1}{N} \qquad (4.2)$$

$\hat{I}$ is not the maximum value $\hat{I}$ of the current flowing through the bumper: each bumper will be powered by a capacitor discharge, and the current i(t) flowing through it varies with time as :

$$i(t) = \hat{I} \sin \omega t \qquad (4.3)$$

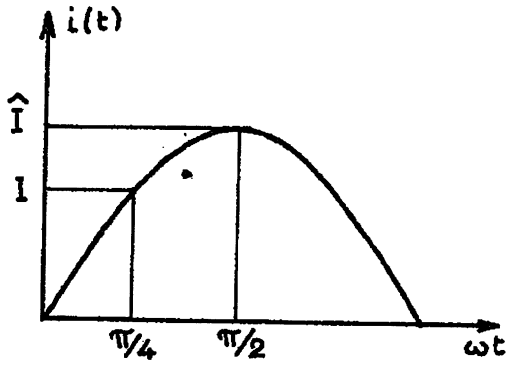

To get a nearly constant beam displacement per revolution, only part of the sine wave can be used. We will take :

$$\hat{I} = I * \sqrt{2} = \frac{B * h}{o} * \frac{\sqrt{2}}{N} \qquad (4.4)$$

There are technical and financial limitations on $\hat{I}$, because of the thyristor switches and of the required number of low-loss transmission cables between the pulse generator in the auxiliary building BA4 and the bumper magnet. According to previous experience (*), and assuming one pulse generator per magnet, we will take, as a reasonable upper limit for $\hat{I}$:

$$\hat{I} \leq 30 \text{ kA} \qquad (4.5)$$

The angular frequency ω of the sine wave is determined by the overall dumping time t_D :

$$\omega = \frac{\pi}{4} * \frac{1}{t_D} \qquad (4.6)$$

t_D is inversely proportional to the beam displacement per revolution, which to a large extent determines the overall efficiency of this dumping process (Chapter 4.4). For the sake of simplicity, we will take t_D equal to

---

(*) G. Gruber, R. Grüb, B. Langeseth, NPA/Int. 69-13

10 SPS revolution times, i.e. 231 μsec, irrespective of the scheme studied. According to Chapter 4.4, this is a convenient value and leads to :

$$\omega = 3.40 * 10^3 \text{ rad/sec} . \tag{4.7}$$

The system impedance is therefore :

$$Z = L\omega \tag{4.8}$$

which gives a magnet voltage:

$$U = \hat{ZI} = L\omega\hat{I} = 4.81 * 10^3 * BN\omega\ell . \tag{4.9}$$

Because of the magnet insulation, which must be radiation resistant and suitable for vacuum of 10^{-7} Torr, this voltage must be restricted to :

$$U \leq 3 \text{ kV}. \tag{4.10}$$

If the required voltage (4.9) turns out to be higher than this limit, the corresponding bumper must be split into 2 or more identical modules, each of them being powered by its own pulse generator. But anyway, because of its mechanical construction and vacuum behaviour, each individual module cannot reasonably be longer than 2.0 m.

4.2 A Bump over one Lattice Period

The best location for the absorber block is in front of a quadrupole, for instance QD 4191. If one wants to avoid aperture problems in the other quadrupoles, the closed orbit bump must be shorter than a magnetic period, i.e. in our example, must be made between QF 4181 and QF 4201. This is achieved with four fast bumpers, as shown in Fig. 4.1. The system is symmetrical with respect to the centre of QD 4191, and the relative strength of each pair of bumpers (K1-K'1, vis. K2-K'2) is adjusted so that a proton, which is not dumped on the absorber block, has

a trajectory in the normalized phase plane as shown in Fig. 4.2. Obviously, to get the minimum strength for the bumpers, K1 (resp. K'1) and K2 (resp. K'2) must be as far apart as possible.

Taking into account the elements already foreseen in the LSS4(*), i.e. correcting dipoles, pick-up stations, octupole lens, leads to the geometrical layout shown in Fig. 4.3, with the absorber block in front of QD 4191 and for 2 m long bumpers. Here again, the aperture at the upstream side of the absorber block is determined by the nominal SPS aperture, i.e :

Full width of the aperture of the absorber block : w = 67.0 mm
Full height : h = 48.0 mm.

Table 4.1 gives the characteristics of the corresponding bumper magnets, for a horizontal and for a vertical closed orbit bump, (see page 20).

Obviously, horizontal dumping is impossible, as both bumpers require too high a number of individual modules. Vertical dumping must be discarded also: although the bumpers K1 and K'1 are split into 2 modules each, which makes this system very expensive (see Appendix II), their magnetic field is rather high and the magnet coils have too many turns which leads to mechanical problems. Also the efficiency of such a system would be rather poor. The voltages in Table 4.1 are calculated assuming that the beam is dumped in 10 SPS revolutions, which means a beam displacement of 4.8 mm per revolution. With the computer programme described in Chapter 4.4, one can calculate that for a beam of vertical betatron amplitude of 4.3 mm at (β_V)max, which is the assumed value at 400 GeV/c(**), 19.5% of the protons will fall on the first millimetre of the edge of the absorber block. As it will be seen in Chapter 5.2, the resulting dumping efficiency will only be about 90%. A 95% efficiency requires doubling the rate of beam displacement per revolution, which implies doubling also the number of

---

(*) Drawing No. 8002-010-1C

(**) The 300 GeV Programme, CERN/1050

Table 4.1

Beam displacement in front of the absorber block		Horizontal 67 mm		Vertical 48 mm	
		K1	K2	K1	K2
Deflection angle	(mrad)	4.54	5.93	2.68	1.36
Mag. strength $\int Bd\ell$ at 400 GeV/c	(T.m)	6.05	7.91	3.58	1.81
Overall magnetic length ℓ	(m)	4.0	4.0	2.0	2.0
Magnet gap width w	(mm)	126.	110.	28.	75.
Magnet gap height h	(mm)	28.	45.	124.	75.
Magnetic induction B	(Tesla)	1.51	1.98	1.79	0.91
Nominal NI value	(kA-turn)	33.7	70.8	176.7	54.2
Number of turns	-	2	4	9	3
Maximum current $\hat{I}$	(kA)	23.8	25.0	27.8	25.6
Number of modules	-	3	6	2	1
Module inductance L	(μH)	30.2	32.8	23.0	22.6
System impedance Z	(Ω)	0.103	0.112	0.078	0.077
Module voltage U	(kV)	2.44	2.78	2.17	1.97

modules for both K1 and K2, and increasing accordingly the cost of such a system.

The absorber block can also be located in front of QF 4181. In this case, the bumper K'1 can be closer to QD 4191, and hence K1 closer to QD 4171, because there is no octupole lens in front of QD 4191. This gives the geometrical layout of Fig. 4.4. The apertures at the upstream side of the absorber block are now :

full width of the aperture w = 117 mm
full height h = 25 mm.

Again, the beam can be dumped horizontally or vertically, and the corresponding bumper characteristics are summarized in Table 4.2.

Table 4.2

Beam displacement in front of the absorber block		Horizontal 117 mm		Vertical 25 mm	
		K1	K2	K1	K2
Deflection angle	(mrad)	6.11	2.85	1.29	1.83
Mag. strength $\int Bd\ell$ at 400 GeV/c	(T.m)	8.14	3.80	1.72	2.43
Overall magnetic length ℓ	(m)	4.0	2.0	2.0	2.0
Magnet gap width w	(mm)	70.	154.	50.	60.
Magnet gap height h	(mm)	50.	30.	65.	120.
Magnetic induction B	(Tesla)	2.04	1.90	0.86	1.22
Nominal NI value	(kA-turn)	81.0	45.4	44.6	116.3
Number of turns	-	4	2	2	6
Maximum current $\hat{I}$	(kA)	28.6	32.1	31.5	27.4
Number of modules	-	4	2	1	2
Module inductance L	(μH)	28.1	25.8	7.7	22.6
System impedance Z	(Ω)	0.096	0.088	0.026	0.077
Module voltage U	(kV)	2.74	2.82	0.828	2.11

Again, horizontal dumping requires too many modules, while vertical dumping would lead to a dumping efficiency which would be even worse than in case of Table 4.1, as the voltages are calculated for a nominal beam displacement of 2.5 mm per revolution. But here the task of the bumpers can be made easier by locating K1 upstream of QD 4171 and K'1 downstream of QD 4191, K2, K'2 and the absorber block being unchanged: see Fig. 4.5, in which K1 (resp. K'1) is kept close to QD 4171 (resp. QD 4191) to avoid aperture problems in the D quadrupoles. (In case of the absorber block in front of QD 4191, the same arrangement cannot be used, as there is no place left for K'1 downstream QF 4201.) With this layout, the bumper characteristics become :

Table 4.3

Beam displacement in front of the absorber block		Horizontal 117 mm		Vertical 25 mm	
		K1	K2	K1	K2
Deflection angle	(mrad)	3.51	1.00	1.1	1.41
Mag. strength $\int Bd\ell$ at 400 GeV/c	(T.m)	4.68	1.33	1.46	1.88
Overall magnetic length ℓ	(m)	3.0	2.0	2.0	2.0
Magnet gap width w	(mm)	65.	150.	50.	60.
Magnet gap height h	(mm)	50.	30.	65.	120.
Magnetic induction B	(Tesla)	1.56	0.67	0.73	0.94
Nominal NI value	(kA-turn)	62.1	15.9	37.9	90.0
Number of turns	-	3	1	2	5
Maximum current $\hat{I}$	(kA)	29.3	22.5	26.8	25.5
Number of modules	-	2	1	1	1
Module inductance L	(μH)	22.1	12.6	7.73	31.4
System impedance Z	(Ω)	0.075	0.043	0.026	0.107
Module voltage U	(kV)	2.20	0.961	0.705	2.72

It will be seen in Chapter 4.4 that the rate of beam displacement must be at least 10 mm/revolution in order to get a reasonable dumping efficiency. Therefore for vertical dumping, the bumpers K2 and K'2 should be split into 4 modules to cope with this rate of displacement and with the voltage limit, making this scheme far too expensive.

Horizontal dumping would give a better dumping efficiency, but this scheme, although feasible, is less attractive than the system using a closed orbit bump over two periods and which will be examined in Chapter 4.3 because :

i) it is more expensive (see Appendix II)

ii) it also leads to aperture problems in the intermediate QD for large beams : at the downstream side of QD 4171 the beam

is already displaced by 18 mm and an enlarged QD would be needed to avoid beam losses.

Therefore horizontal dumping with four bumpers is no longer considered in this report.

4.3 Bump over Two Lattice Periods

The only way to reduce the requirements on the bumpers is to increase the length of the closed orbit bump, i.e. to increase the distance between K1 and the absorber block.

For a given Q-value, one can find locations for the two bumpers K1 and K'1 for which the betatron phase shift in between is just 180°. In this case, the bumpers K2 and K'2 are no longer needed. If, however, the Q-working point of the SPS is changed, the magnets are no longer half a betatron wavelength apart, which results in a coherent betatron oscillation around the SPS ring with an amplitude determined by the Q-change.

Under certain conditions this may lead to some beam blow-up during the dumping process and to undesirable beam loss on the elements like the electrostatic septum or the other septum magnets. The Q dependence of this scheme can be corrected by placing a third bumper K2 half way between K1 and K'1. The resulting particle trajectory in the normalized phase plane is shown in Fig. 4.6, in which the absorber block is upstream and K2 immediately downstream of QF 4181.

The betatron phase angle between K1 and K'1 varies linearly with Q to a first approximation. Because of the relatively small range of variation for the Q-working point, the strength of K2 will be small as compared to those of K1 and K'1. We will therefore disregard K2 in the first assessment of this scheme and assume that Q = 27.75 exactly. The effect of a Q-change will be examined in Chapter 4.4.

For the absorber block in front of QF 4181, the geometrical layout is given in Fig. 4.7. The magnet length can conveniently be chosen as 2.0 m. Because of the aspect ratio of the bumper magnets, only horizontal dumping can be considered.

One could also imagine to place the absorber block in front of QD 4191, but then the only location for K'1 is in the short straight section upstream to QD 4211. This has the disadvantage that part of the closed orbit bump takes place outside the long straight section. Moreover, the available straight section length limits the length of the bumper K'1, which leads to higher currents than for the case of the absorber block in front of QF 4181, although the beam displacement in front of the absorber block would be smaller. Therefore, this latter layout is disregarded.

The aperture at the upstream side of the absorber block, when in front of QF 4181, is the same as in the previous paragraph :

full width of the aperture w = 117 mm
full height h = 25 mm.

Both magnets K1 and K'1 have the same aperture. Their characteristics are given in Table 4.4, and are such that this system is technically feasible. The choice between a single-turn or a two-turn magnet would result, after prototype work, from the best compromise between lowest current and lowest voltage, but it is not necessary to split K1 and K'1 into small modules.

Table 4.4

Beam displacement in front of the absorber block	Horizontal 117 mm	
Deflection angle for K1	1.32 mrad	
Mag. strength $\int Bd\ell$ at 400 GeV/c	1.762 T.m	
Magnet length ℓ	2.0 m	
Magnet gap width w	1.34 mm	
Magnet gap height h	28. mm	
Magnetic induction B	0.881 Tesla	
Nominal NI value	19.6 kA	
Number of turns	1	2
Maximum current $\hat{I}$	27.7 kA	13.9 kA
Magnet inductance L	12.0 µH	48.1 µH
System impedance	0.041 Ω	0.164 Ω
Voltage U	1.13 kV	2.27 kV

4.4 System Efficiency

In the scheme described in Chapter 4.3, the displaced beam has to pass through the intermediate quadrupole QD 4171, and it must be checked if protons are lost on its vacuum chamber during the dumping process. One has also to find the best rate of beam displacement per revolution and the number of revolutions necessary to dump all the beam, as well as the proton distribution on the front face of the absorber block, in order to assess the efficiency of this dumping system.

This was done by computer simulation. For a given set of parameters (location of the elements, Q-value, momentum spread, beam size and distribution in the transverse phase plane), a particle is chosen randomly, and its trajectory in the radial phase plane is tracked until the particle is dumped or lost elsewhere outside the machine aperture. Statistics are then collected for about 8000 particles per case.

The following parameters were varied :

a) Q-value :

b) rate of beam displacement per revolution ;

c) particle distribution in the transverse phase plane: gaussian-like and uniform distribution, this latter representing the worst case;

d) half beam width. Three values, given here at (β_H)max, were used:

i) 6.2 mm, which corresponds to the assumed beam width at 400 GeV/c (see CERN/1050)

ii) 27.6 mm, which corresponds to the beam emittance at injection, for bunch-by-bunch transfer from CPS to SPS

iii) 57.5 mm, which is the half width of a beam filling completely the SPS aperture, taking into account a maximum horizontal closed orbit deviation of 10 mm at (β_H)max.

The results given below are for a uniform particle distribution in the radial phase plane, and for a nominal Q-value of 27.75. To characterize the particle distribution on the absorber block in front of QF 4181, we give in Table 4.5 the percentages of protons which are dumped within the first millimetre of the absorber block front face. As discussed in Chapter 5.2, these percentages determine the efficiency of the absorber block, as these protons or their secondaries have a high probability to escape from the absorber block. The number n of revolutions necessary to dump the whole beam is also given.

Table 4.5

Half beam width at (β_H)max = 109.2 m	Horizontal beam displacement in mm/revolution					
	5		10		20	
	% on 1st mm	n	% on 1st mm	n	% on 1st mm	n
6.2 mm	14.6	14	9.6	8	4.9	5
27.6 mm	8.2	14	5.5	8	4.1	5
57.5 mm	6.6	14	4.1	8	2.8	6

The percentages given in Table 4.5 do not depend very much on Q. To the contrary, the number of required revolutions can be higher than the figures given above, for Q-values close to 28.0 and especially for a rate of beam displacement of 5 mm/revolution (n up to 24).

It will be shown in Chapter 5.2 that for protons which are falling within 1 mm from the edge of the absorber block, about 50% of the corresponding energy escapes through the aperture of the absorber block, irrespective of the momentum of the primary protons. This makes it necessary to choose the rate of beam displacement per revolution sufficiently high in order not to reduce the dumping efficiency too much.

On the other hand, if the beam displacement is too fast, protons are lost in the aperture of QD 4171 during the dumping process. Table 4.6 gives the maximum position of the deflected protons, in real millimetres, at the downstream side of QD 4171 just before dumping. In parentheses are given the percentages of particles lost at this QD, for a standard quadrupole, taking into account a clearance of only 3 mm bebetween the beam and the vacuum chamber of the quadrupole, since horizontal closed orbit control in LSS4 up to 400 GeV/c is foreseen by means of slow bumpers for beam scraping.

Table 4.6

Half beam width at (β_H)max = 109.2 m	Horizontal beam displacement in mm/revolution		
	5	10	20
6.2 mm	28(-)	30(-)	34(-)
27.6 mm	34(-)	40(0.25%)	48(8.6%)
57.5 mm	38(0.01%)	45(5.6%)	≥57(29.8%)

These beam displacements are calculated assuming a perfect vertical closed orbit. Also,if there is a vertical closed orbit deviation of

5 mm in QD 4171, the beam excursions in this QD will be limited when driving the beam horizontally. This was not taken into account in Table 4.5, and the corresponding percentages are somewhat optimistic.

To avoid these beam losses, the quadrupole QD 4171 must be enlarged. As it is shown in Appendix IV, the largest beam can pass through a quadrupole similar to the ones foreseen for slow extraction, when the rate of beam displacement is 10 mm/revolution. For 20 mm/revolution, there are still losses even for an enlarged QD. Therefore 10 mm/revolution is the best compromise between beam losses and absorber block efficiency. For this rate of beam displacement, an additional absorber block in front of QD 4171 to protect it would not be needed, but is necessary as a protection in case of a faulty tracking of the amplitude of the closed orbit bump with the proton energy.

5. Beam Dump Absorber Block

5.1 Description

The beam dump block will consist of a cylindrical metal block installed at the downstream side of a straight section. During the acceleration, the beam will pass through a rectangular hole in the centre of the block. For dumping, the beam will be kicked vertically or horizontally onto the front surface so that the protons and their subsequent cascade particles are absorbed in the dump block material.

With 10^{13} protons per pulse at 400 GeV/c the kinetic energy of the circulating beam is 160 kcal/pulse and this requires a good heat conductivity of the dump block material and a water cooling of the block.

The total weight of the block is limited to 25 tons by the maximum load capacity of our means of transport. A dump block of such a weight and, as explained later, consisting of a copper-beryllium core surrounded by iron, will be about 4 m long and will have a diameter of 1 m. This is sufficient to absorbe the cascade to nearly 100%, except for the protons and cascade particles escaping out of the inner hole, and to provide sufficient self-shielding. For 400 GeV/c protons, the energy density deposited at 15 cm inside the copper block is estimated to be 55 MeV/g*), The lateral spread of the cascade at this depth can be neglected, so that the local heating and the resulting thermal stresses are determined by the horizontal and vertical proton density distributions within the primary beam. In case of dumping with a fast kicker system and assuming a constant population in the horizontal and vertical phase planes with half beam sizes at $(\beta)_{max}$ of horizontally 6.2 mm and vertically 4.3 mm **), the local instantaneous temperature rise inside the block is about 400°C for 10^{13} protons/pulse at 400 GeV/c. For Gaussian-like beam shapes, it might go up to 1000°C.

*) J. Ranft, LAB II/RA/Note/71-10.
**) The 300 GeV Programme, CERN 1050

If the same beam is spread over the front of the absorber block in the case of dumping the beam by a closed orbit bump over several revolutions, the same calculation gives a local instantaneous temperature rise of 325° C for a constant phase plane population and about 550°C for a Gaussian-like distribution.

In addition to these temperature spikes, there is a time average temperature difference of the order of 200°C between the inner part and the outer wall of the copper cylinder, which is determined by the steady state heat flow of 100 kW to the outside of the block. At 200 GeV/c, these temperature increases are expected to be smaller by a factor of about 2.5.

The above mentioned facts show that additional effort is needed to cope with the severe thermal problems involved in dumping a low emittance beam of 10^{13} protons/pulse at 400 GeV/c. It can be envisaged to reduce the proton density by blowing up a small beam by means of a pulsed quadrupole or the kickers for the Q-measurements. However, this is not compatible with fast emergency beam dumping when required. Another possibility in case of vertical dumping with a fast kicker system, is to sweep the beam horizontally over the front of the dump by means of a kicker excited by a capacitor discharge, and placed downstream of the other kicker magnets. We tend to believe that the technical solution is easier for dumping with a fast kicker system rather than for dumping with a bumper system, since the handling of a blown up beam during dumping over several revolutions is much more difficult.

Figure 5.1 shows a tentative sketch of the beam dump block. The inner part is a core of beryllium-copper. This material represents a reasonable compromise between good nuclear absorption, good thermal and mechanical characteristics, easy machining and low cost.

5.2 Nuclear Cascade Calculations

5.2.1 Definitions and General Remarks

We define the dump efficiency as the ratio of the energy absorbed in the dump block, to the energy which enters the dump block. For the evaluation of the total efficiency of a dumping system, the losses elsewhere in the machine due to the dumping process must be added. The dump efficiency is determined by the following effects :

(a) Outscattering of primary protons, which are incident on the front surface of the dump.

(b) Outscattering of primary protons which are incident on the face of the dump aperture, due to the misalignment of the dump or to non-zero impact angles.

(c) Shower particles, created by protons incident on the front surface, which escape at the face of the dump aperture and the end of the block.

(d) Shower particles, created by protons hitting the face, which escape again at the face of the dump aperture or at the end of the block. We shall only treat here the case of a misalignment shown in the figure which is the most pessimistic case.

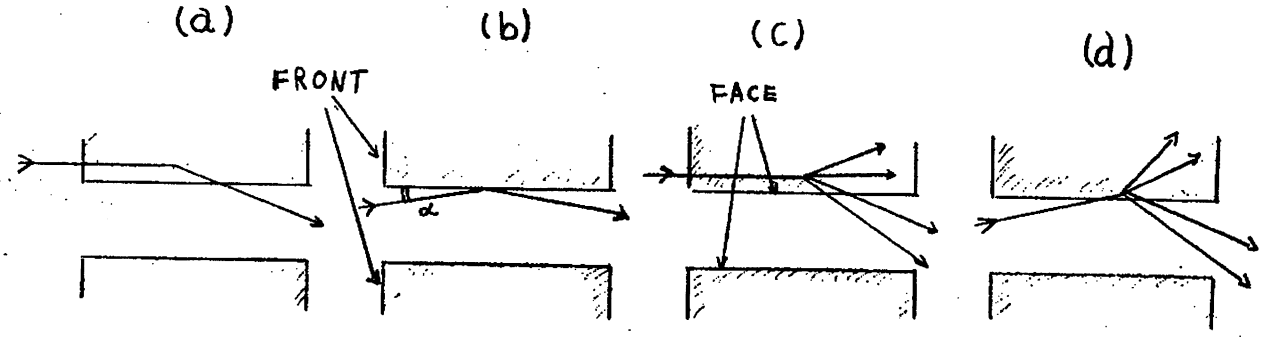

For the computation of the case (a) and (b) Monte-Carlo methods have been applied which take into account coulomb-scattering, nuclear elastic and nuclear quasi-elastic scattering. The scattering cross sections

and angles were taken from Ref. *), which were measured at 19.3 GeV/c and scaled for higher energies **). This may introduce a systematic error of up to 50% into the results obtained for the above mentioned effects (a) to (d). However, for the comparison of the dump efficiencies at different energies and geometries, the results should be reliable. The cases (c) and (d) were treated with Monte-Carlo programmes FLUKA and MAGKA ***). The above arguments for the involved errors apply also in these cases.

5.2.2 Results of Monte-Carlo Calculations

The results are presented in the following figures:
Figure 5.2 shows the cases (a) and (c) for momenta of 50 and 200 GeV/c and for different sizes of a cylindrical hole in the copper dump block with a length of 4 metres. The total escape probability w(x) of the incoming proton energy is plotted, assuming normal incidence, as a function of the impact distance x from the dump block edge. It shows that the critical distance for the outscattering of primary protons is always smaller, due to the small scattering angles, than the one for the cascade particles,which have larger average angles. The hole diameter of 2 or 12 cm has a larger influence on the escape of a 50 GeV/c cascade than that of a 200 GeV/c cascade, again due to larger average angles in the cascade for lower primary momenta. The total percentage of escaping energy $W_{(a) + (c)}$ of effects (a) and (c) is given by

$$W_{(a) + (c)} = \int_0^\infty \rho(x)\, w(x)\, dx \approx \bar{\rho} * \int_0^\infty w(x)\, dx = \bar{\rho} * T_{(a) + (c)}$$

$\rho(x)$ is the percentage of beam per mm arriving at the dump front.

---

*) G. Belletini et al, Proton-nuclei cross-sections at 20 GeV/c, Nuclear Phys. 79, 609 (1966).

**) Radiation Problems encountered in the Design of Multi-GeV Research Facilities CERN 71-21, Laboratory II, Radiation Group, 29 September, 1971.

***) J. Ranft and J.T. Routti, CERN LAB II/RA/71-4

It is an approximately constant value $\bar{\rho}$ over the x interval of interest in case of dumping by a closed orbit bump system. The magnitude T is used later to compare different systems independently of the incoming density $\bar{\rho}$.

The amount $W_{(b)}$ of escaping primary protons due to effect (b) is given by

$$W_{(b)} = \int_0^{\alpha \cdot L} \rho(x)\ \varepsilon(\alpha)\ dx \approx \bar{\rho} * \varepsilon(\alpha) * \alpha * L = \bar{\rho} * T_{(b)}$$

α : angle of misalignment

L : dump block length

$\varepsilon(\alpha)$: escape probability for primary protons hitting the dump face under an angle α

The magnitude $T_{(b)}$ is plotted in Fig. 5.3 as a function of α. The curves go through a maximum, since $\varepsilon(\alpha)$ is again small for large misalignments.

As the average angles under which secondaries are emitted are large compared to the possible misalignments, of say up to 0.3 mrad, we can assume that the escape probability δ for the cascade (effect (d)), is independent of the misalignment α. The amount of escaping cascade particles $W_{(d)}$, created by protons hitting the face becomes :

$$W_{(d)} = \int_0^{L \cdot \alpha} \rho(x) * \delta * \left[1 - \varepsilon(\alpha)\right] dx \approx \bar{\rho} * L * \alpha * \delta * \left[1 - \varepsilon(\alpha)\right] = \bar{\rho} * T_{(d)}$$

As shown in Fig. 5.3, we find a linear rise of $T_{(d)}$ after $\varepsilon(\alpha)$ has become small.

5.3 Dump Efficiency

The above mentioned programmes can only treat dumps with round holes. But the actual hole has a rectangular shape of 25 x 117 mm for a dump placed in front of a QF. The corresponding value of T is calculated in

the following way for the dumping system by a closed orbit bump.

$$T \text{ (rectangular hole)} = \frac{3 * T\ (\phi = 2) + 1 * T(\phi = 12)}{4}$$

Summing up all contributions

$$T_T = T_{(a) + (c)} + T_{(b)} + T_{(d)}$$

we obtain the following table :

Table 5.1

	$T_{(a) + (c)}$	$T_{(b)} + T_{(d)}$	$T_{(b)} + T_{(d)}$	T_T	
Misalignment:		α = 0.1 mrad	α = 0.3 mrad	α = 0.1 mrad	α = 0.3 mrad
P = 50 GeV/c	8×10^{-2}	27×10^{-2}	57×10^{-2}	35×10^{-2}	65×10^{-2}
P = 200 GeV/c	9×10^{-2}	20×10^{-2}	43×10^{-2}	29×10^{-2}	52×10^{-2}

One might arrive at values which are somewhat pessimistic by summing up cases (a) and (b), since in the calculations for the first column no misalignment is assumed. But this effect can be neglected within the accuracy of these estimates.

These values in Table 5.1 must now be multiplied with the density $\bar{\rho}$ (see chapter 4.4, table 4.5) arriving at the dump edge, to obtain the total dump loss W_T given in Table 5.2, for the case of dumping by a c.o. bump system.

Table 5.2

Total Dump loss [%]

P [GeV/c]	Half Beam Size [mm]	Beam Displacement [mm/revolution]					
		5		10		20	
		0.1 mrad	0.3 mrad	0.1 mrad	0.3 mrad	0.1 mrad	0.3 mrad
50	57.5	2.3	4.3	1.4	2.7	1.0	1.8
200		1.9	3.4	1.2	2.1	0.8	1.5
50	27.6	2.9	5.3	1.9	3.6	1.4	2.7
200		2.4	4.3	1.6	2.9	1.2	2.1
50	6.2	5.1	9.4	3.4	6.2	1.7	3.2
200		4.2	7.6	2.8	5.0	1.4	2.5

The two different values in each line are for misalignments of the dump block of respectively 0.1 mrad and 0.3 mrad. These values give also the total escape of the whole $\lambda/2$-dumping system since, apart from some extreme cases, no protons are lost in the aperture without having touched the dump. The efficiency of this system is thus defined entirely by the dump efficiency. It can be somewhat improved by putting an additional stopper at the end of the next half period straight section, with an enlarged vacuum pipe in between, so that part of the escaping shower particles will be caught there.

For the fast kicker system,the dump efficiency is always very high, since the amount of protons arriving near the dump corner is of the order of 1 $^{o}/_{oo}$ for a time constant of the kick strength of 0.4 μsec. But contrary of the $\lambda/2$ system, the loss of protons kicked into the aperture of the SPS is about 1 %, i.e. the efficiency of the fast kicker system is mainly determined by the system efficiency.

6. Conclusions

It has been shown that among the alternative dumping schemes discussed in this report, only two systems are of interest in view of their technical feasibility and their cost. One dumping scheme uses two fast kicker magnets downstream of QD 4171 which give the beam during one revolution a constant vertical deflection onto the beam dump absorber block upstream of QD 4191. The other dumping scheme uses a growing half wave length bump, generated by two magnets which each are placed at either end of LSS 4. This bump displaces the beam radially onto an absorber block placed upstream of QF 4181 at a rate of about 10 mm per revolution.

In both schemes the deflected beam passes through the aperture of a quadrupole situated between the magnet(s) and the absorber block. It has been shown for both systems that this must be an enlarged quadrupole of the type planned for use in the extraction straight sections LSS 2 and LSS 6. This quadrupole is for the fast dumping scheme QF 4181 and for the bumping scheme QD 4171. Moreover, due to the need of a matched lattice, also QF 4161 respectively QD 4191 should be of the enlarged type.

We propose to adopt the fast kicker scheme for internal dumping in the SPS, in spite of its higher cost as compared with the half wave length bump system, for the following reasons :

i) We intend for both systems to place the magnets in vacuum tanks. With laminated magnets there are problems with outgassing due to the thin laminations of the yoke and the epoxy insulated coil. Moreover, due to the latter, these magnets cannot be prebaked in order to achieve a good vacuum. On the other hand, the ferrite magnets for the fast kicker system do not contain any organic material and can be prebaked if necessary.

ii) There is little experience with the technology of laminated bumper magnets with an epoxy insulated coil, which operate in vacuum, and which are excited by fast pulses with heavy currents

and voltages of a few kilovolts. The mechanical shock during the pulse may cause wear of the insulation which will decrease the voltage holding capability of the epoxy and which will diminish the reliability of the system.

iii) The performance of the fast kicker system is straightforward and practically independent of the choice of Q value, since it dumps the beam in one revolution. The bumping system uses about eight revolutions and its performance is more dependent on the Q-value. We may need a third bumper magnet downstream of QF 4181 in order to compensate for Q-changes and to avoid blow-up of the beam during the dumping process.

iv) The fast kicker system offers the advantage of a straightforward extension which can sweep a beam of low emittance and high intensity over the front surface of the dump block in order to decrease the thermal problems of the latter. This technique is compatible with emergency beam dumping when the latter is required.

v) For beam dumping at injection or at high proton momenta of beams of normal emittance, and under normal operating conditions, the total amount of beam energy lost outside the absorber block is about 1% for the fast kicker scheme and, depending on conditions, 2% to 5% for the bumping scheme. Moreover, these last figures for the bumping scheme are estimates which may be wrong by 50 %.

Acknowledgements

We have profitted from enlightening discussions with several colleagues among whom we want to mention in particular Y. Baconnier and K.H. Kissler.

APPENDIX I

Cost estimate for fast kicker systems

The following systems are costed in kSF:

- vertical dumping with 4 kicker magnets, 4 m length each, as described in Table 3.1 (kick over half a lattice period),
- vertical dumping with 2 kicker magnets, 2.5 m long each, as described in Table 3.2 (kick over a lattice period).

	Kick over ½ period with 4 kickers		Over 1 period with 2 kickers	
	per item	total	per item	total
1) Kicker magnet				
ferrite for C-shape magnet	60		45	
mechanical parts	112		70	
vacuum tank	128		80	
pumps and gauges	120		75	
	420	1680	270	540
2) Pulse forming network				
condensors 60 kV, 4μF total	130		130	
PFN tank with pyralene	100		100	
thyratron tank	40		40	
thyratron 10 kA, 60 kV	16		16	
transmission cable + connectors	30		30	
terminating resistor	35		35	
controls and interlocks	15		15	
	366	1464	366	732

	over ½ period with 4 kickers		over 1 period with 2 kickers	
	per item	total	per item	total
3) power supply				
HV power supply, 60 kV	90		60	
controls and interlocks	40		30	
current divider	30		15	
	160	160	105	105
4) Installation and commissioning				
Faraday cage, scope, electronics	90		80	
Installation and cabling	120		100	
	210	210	180	180
5) Absorber block				
absorber block, 4 m long	200	200	200	400
beam stopper		50		50
cost for enlarged quadrupoles				250
6) Spares and prototype work				
Magnet prototype + vacuum tank	420			
pulse forming network	370		370	
power supply	90		60	
electronics	50		50	
	930	930	480	480
Overall Cost		4694		2737

APPENDIX II

Cost estimates for c.o. bump systems

Two systems are costed in kSF :

1. Dumping system by a horizontal c.o. bump over one lattice period, as described in Table 4.3. This scheme requires 4 bumpers, 2 of them being split into 2 modules. The vertical dumping system with 4 bumpers, as described in Table 4.1 would give about the same cost estimate.

2. Dumping system by a horizontal c.o. bump over two lattice periods with 2 bumpers. The correcting bumper for Q-change is costed separately.

	1 period c.o. bump		2 periods c.o. bump	
	per item	total	per item	total
1) Bumper magnet				
laminated magnet	90		80	
vacuum tank	65		65	
pumps and gauges	75		75	
	230	1380	220	440
2) Pulse generator				
condensor	50		30	
transmission cable + connectors	40		40	
thyristors	30		30	
diodes	15		10	
mechanical parts	15		10	
	150	900	110	220
3) Power supply				
3 kV power supply	80		60	
controls and interlocks	60		50	
	140	420	110	110

	1 period c.o. bump		2 periods c.o. bump	
	per item	total	per item	total
4) Installation and commissioning				
Faraday cage, scope + electron.	100		100	
installation and cabling	150		100	
	250	250	200	200
5) Absorber block				
absorber block	200	200	200	400
beam stopper		50		50
cost for enlarged quadrupoles		250		250
6) Correction bumper for Q-change				
bumper magnet + vacuum tank			150	
pulse generator, power supply + controls			60	
installation and commissioning			40	
			250	250
7) Spares and prototype work				
laminated magnet + vacuum tank	230		220	
pulse generator and power supply	220		200	
electronics	50		50	
	500	500	470	470
Overall Cost (kSF)		3950		2390

APPENDIX III

Aperture requirements in the intermediate quadrupole for the fast kicker system

APPENDIX IIIa

Allowance for the vertical c.o. deviation

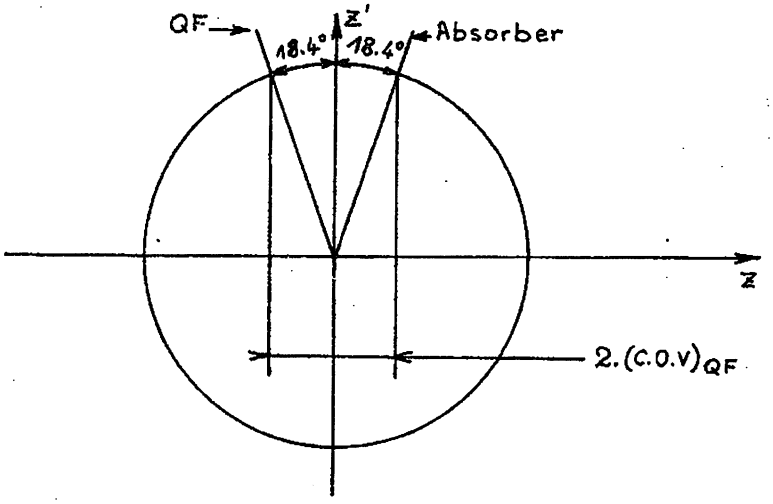

The largest allowance for a vertical c.o. deviation in QF 4181 has to be made when the phase of the c.o. deviation has a value as indicated in the above sketch.

For the vertical phase advance of 36.8° between the downstream side of QF 4181 and the front of the absorber block, one gets :

$$\text{Allowance} = 2 * (\text{C.O.V.})_{QF} = 2 * (\text{C.O.V.})_{max} \left[\frac{\beta_{QF}}{\beta_{max}}\right]^{\frac{1}{2}} * \sin 18.4^{\circ}$$

For $(\text{C.O.V.})_{max} = 5$ mm, the allowance for the vertical c.o. deviation becomes 1.3 mm.

APPENDIX IIIb

Allowance for the deflection during dumping

Figures IIIb.1 and 2 show in the normalized vertical phase plane z, z' the aperture requirements in QF 4181. All values are scaled to (β_V)max. The vertical lines which indicate the vertically available half aperture of the normal and the enlarged QF are valid for the nominal beam size at injection. They include 1.3 mm for c.o. deviations and 1 mm clearance between beam and vacuum chamber.

In Fig. IIIb.1 it is assumed that the protons in the normalized vertical phase plane are deflected at the centre of the kickers with a deflection angle α_N equivalent to the nominal 44 mm displacement at the position of the absorber block 2, i.e. 51 equivalent mm in the normalized phase plane. This block has a phase shift of about 90^o from the centre of the kickers. At the front of absorber block 1, the heavily marked part of the phase space circle can pass through the block, whereas the rest of the circle is intercepted by it.

At the downstream end of QF 4181, the part which has passed through absorber 1 is heavily marked again. The hatched area will fall into a normal QF.

All plots lead to a somewhat pessimistic result, because part of the protons of the hatched area missing the front of the block will still hit the surface of the dump aperture and may stay within the absorber block.

In Fig. IIIb.2, a continuous variation of the deflection angle between α_N and α_M is considered under the same assumptions as in the previous figure, where α_M is just large enough to dump the whole beam on absorber 1. For deflection angles between α_M and α_N, the heavily marked part can again pass the absorber 1 whereas the hatched part hits the vacuum chamber of a normal QF, but can pass through an enlarged QF.

APPENDIX IV

Aperture requirements in the intermediate quadrupole for the bump system

Figure IV.1 shows the normalized horizontal phase plane at the position of the absorber block in consecutive revolutions. All values of this figure are scaled to (β_H)max. (A) indicates the position of the nominal injection beam at an instant within the 4th revolution after the start of horizontal dumping. The heavily marked part of the circle can pass through the absorber block, whereas the dotted part is intercepted by it. (B), (C), (D) and (E) show the situation after one, two, three, four revolutions respectively. Due to Q_H = 27 3/4, the position of the area of the circle which is cut off at each revolution is turned by 90^o at the next revolution.

In Fig. IV.2 the situation (E) is shown again. In addition, the position of this area at the downstream side of QF 4171 is indicated together with the aperture limits in a normal and an enlarged QD. The horizontal aperture limit in the circular vacuum chamber of QD depends strongly on the vertical amplitude of the protons. The verical lines in fig. IV.2 which indicates the half aperture of the normal and enlarged quadrupole are valid for protons with a_z = 19.25 mm and $(COV)_{max} = \pm 5$ mm. Figure IV.2 shows that the beam always passes an enlarged but not a normal QD. One can also see in this figure that a normal QD cannot be completely shielded by an additional absorber block : the last part of the beam, which has to be dumped, passes through the absorber block 1 and part of it falls nevertheless onto the vacuum chamber of the normal QD. This absorber 1 is positioned as stated in Chapter 2.2.

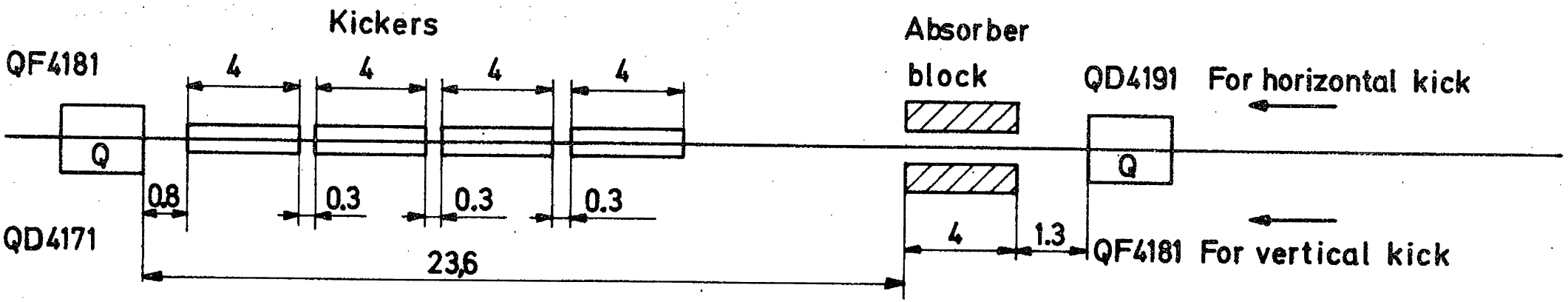

Fig.3.1 Deflection over half a period

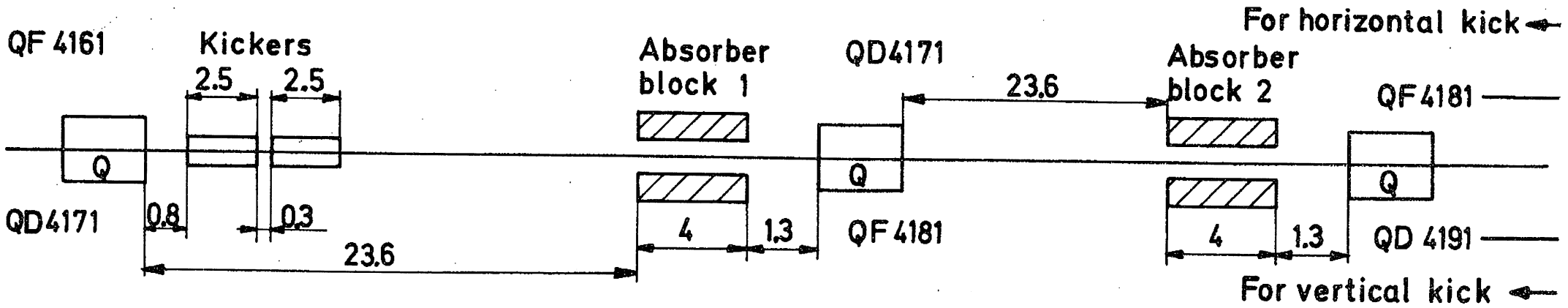

Fig. 3.2 Deflection over one period

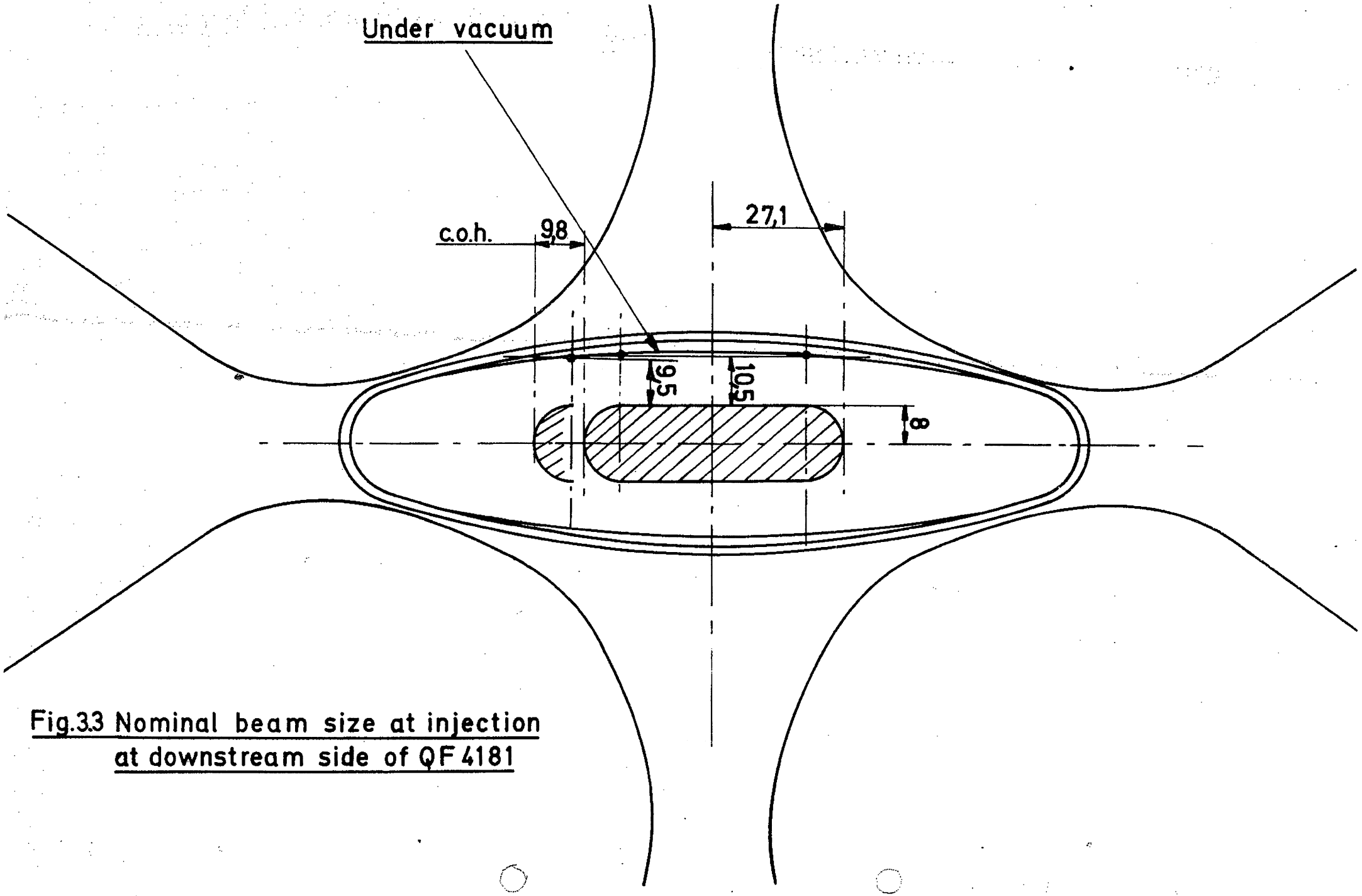

Fig.3.3 Nominal beam size at injection at downstream side of QF 4181

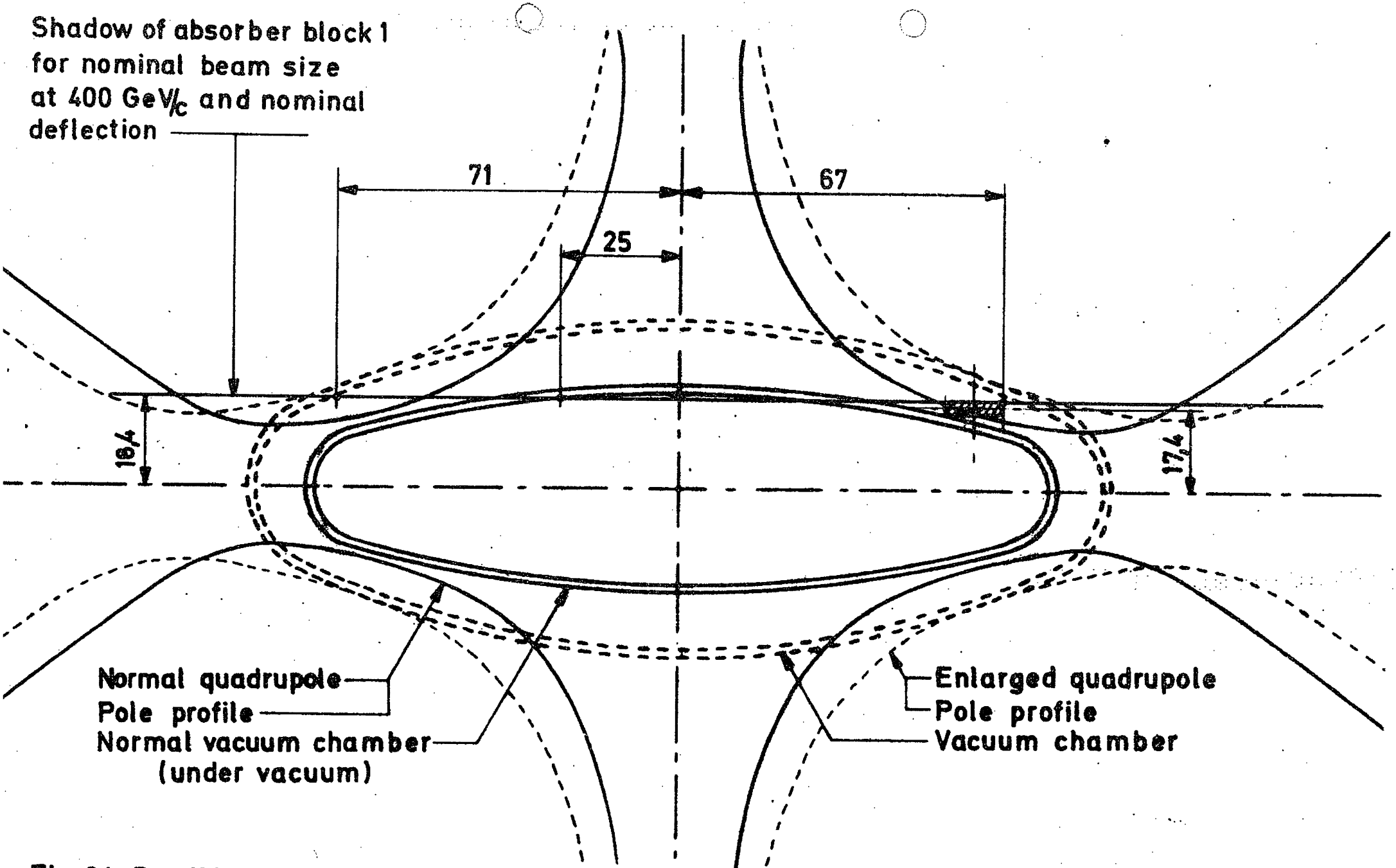

Fig. 3.4 Possible beam excursions in the aperture of QF 4181

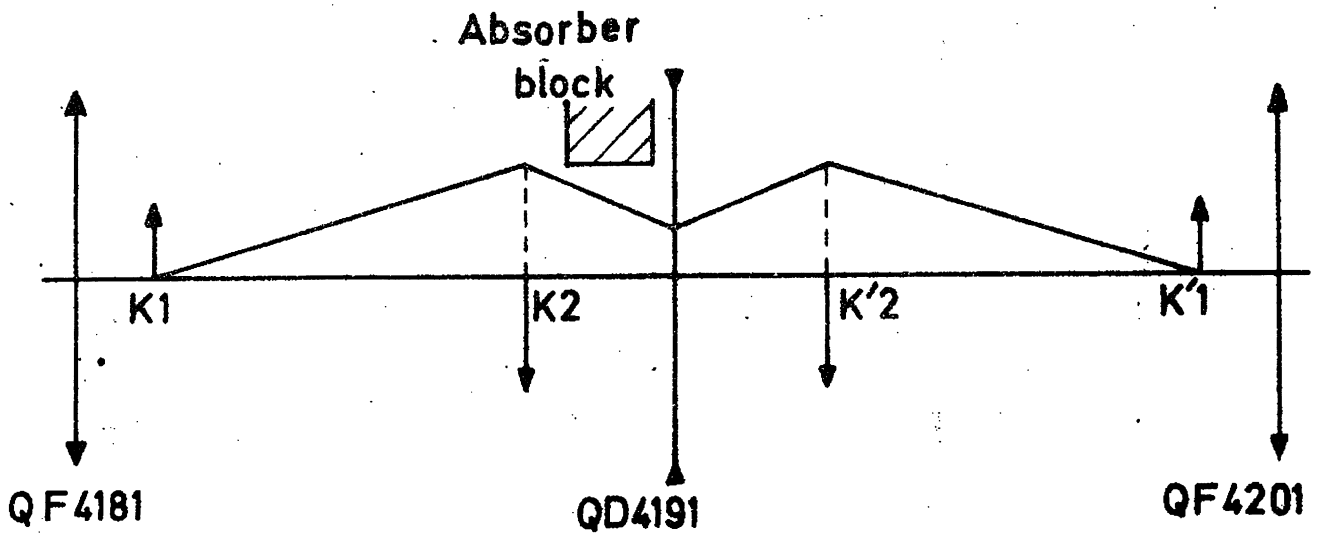

Fig. 4.1 Beam dumping with four bumpers

Fig. 4.2
Particle trajectory in the normalized phase plane

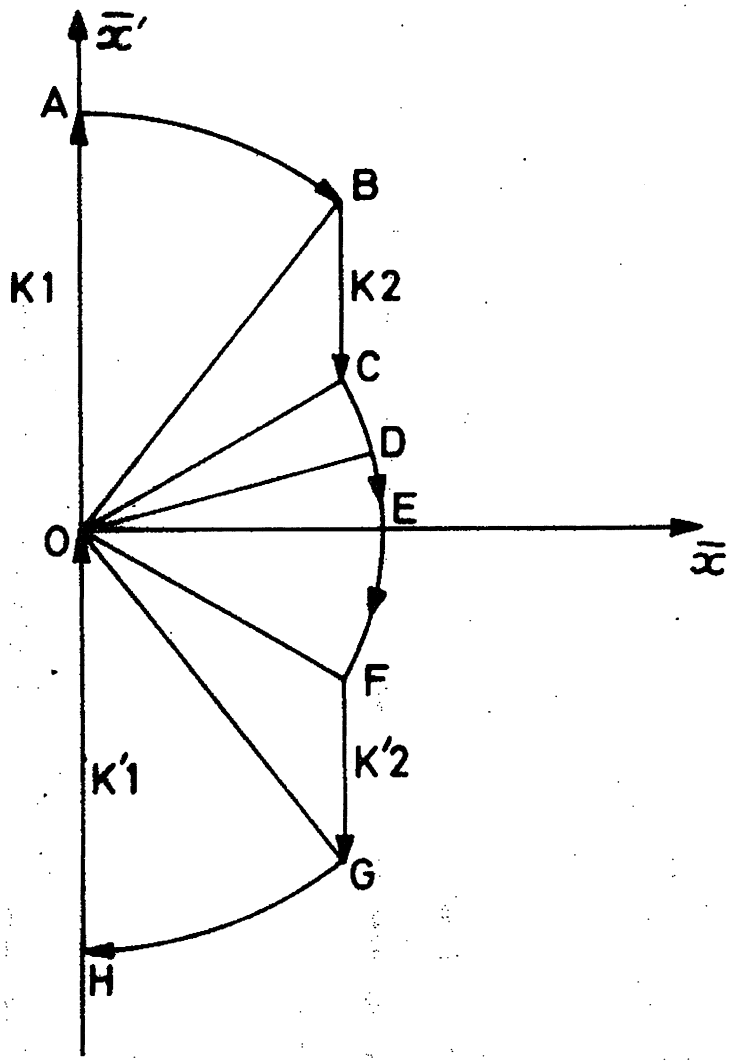

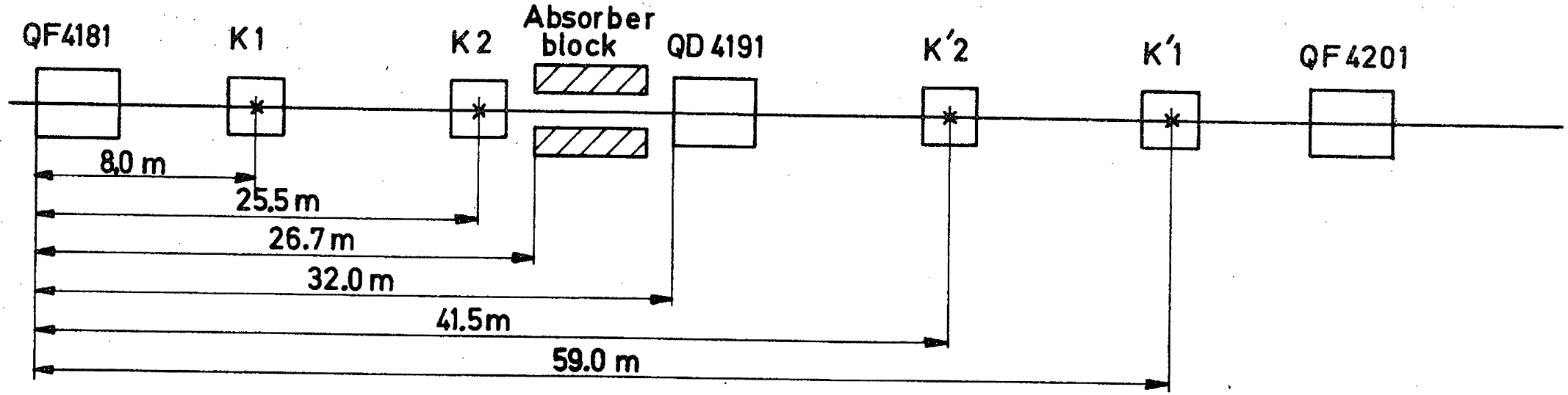

Fig 4.3 Layout for the absorber block in front of QD 4191

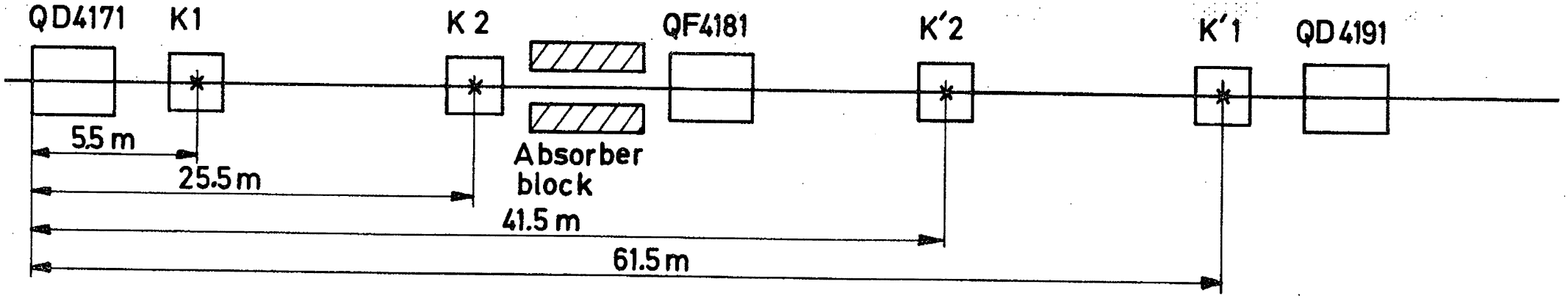

Fig. 4.4 Layout for the absorber block in front of QF4181

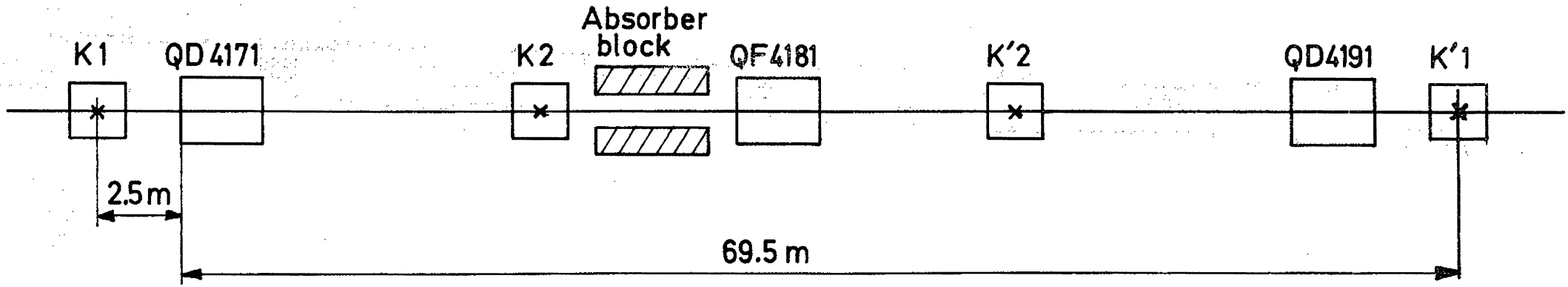

Fig. 4.5 Alternative layout for the absorber block in front of QF 4181

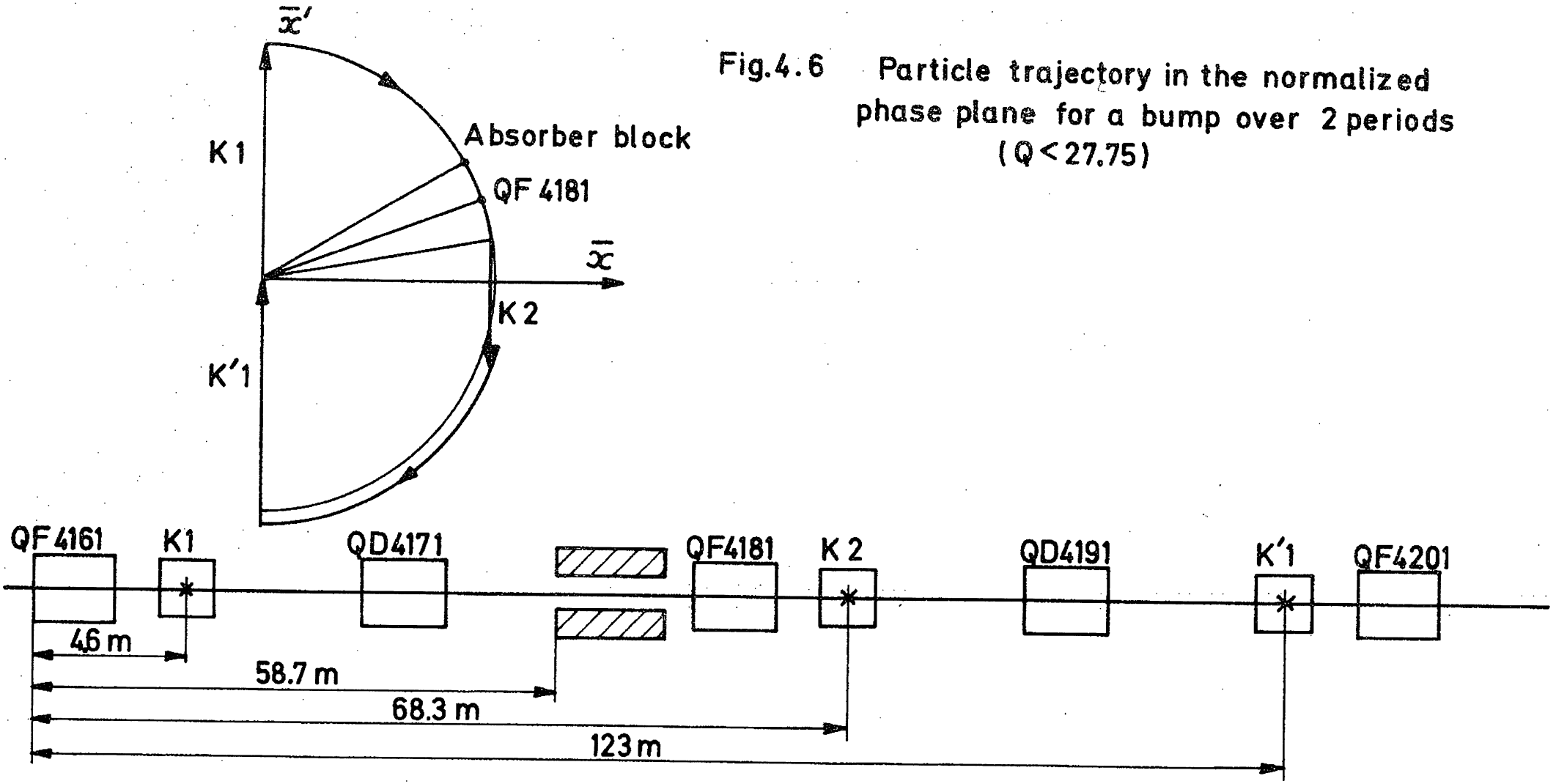

Fig.4.6 Particle trajectory in the normalized phase plane for a bump over 2 periods ($Q < 27.75$)

Fig 4.7 Geometrical layout for a bump over 2 periods

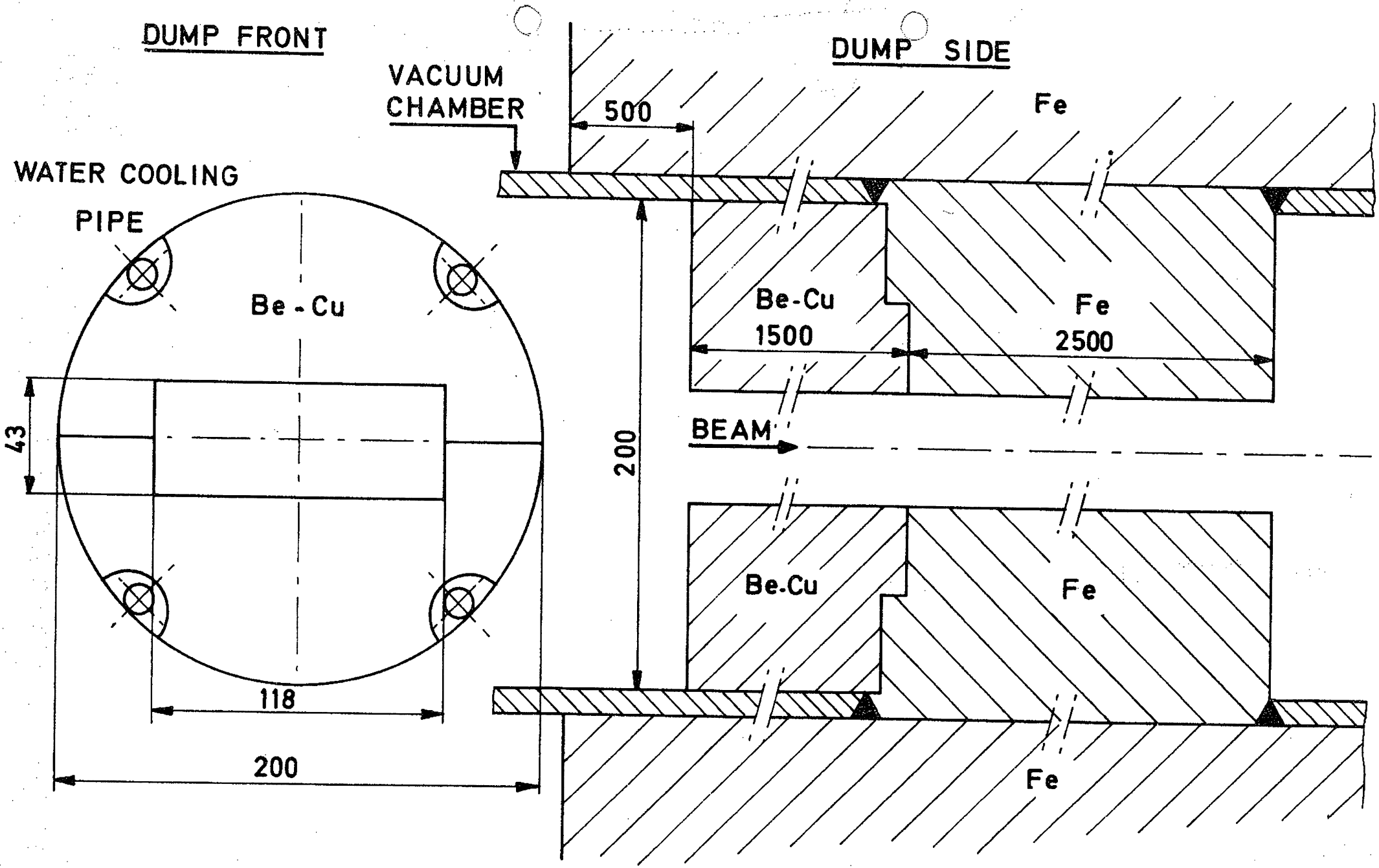

Fig. 5.1 BEAM DUMP BLOCK

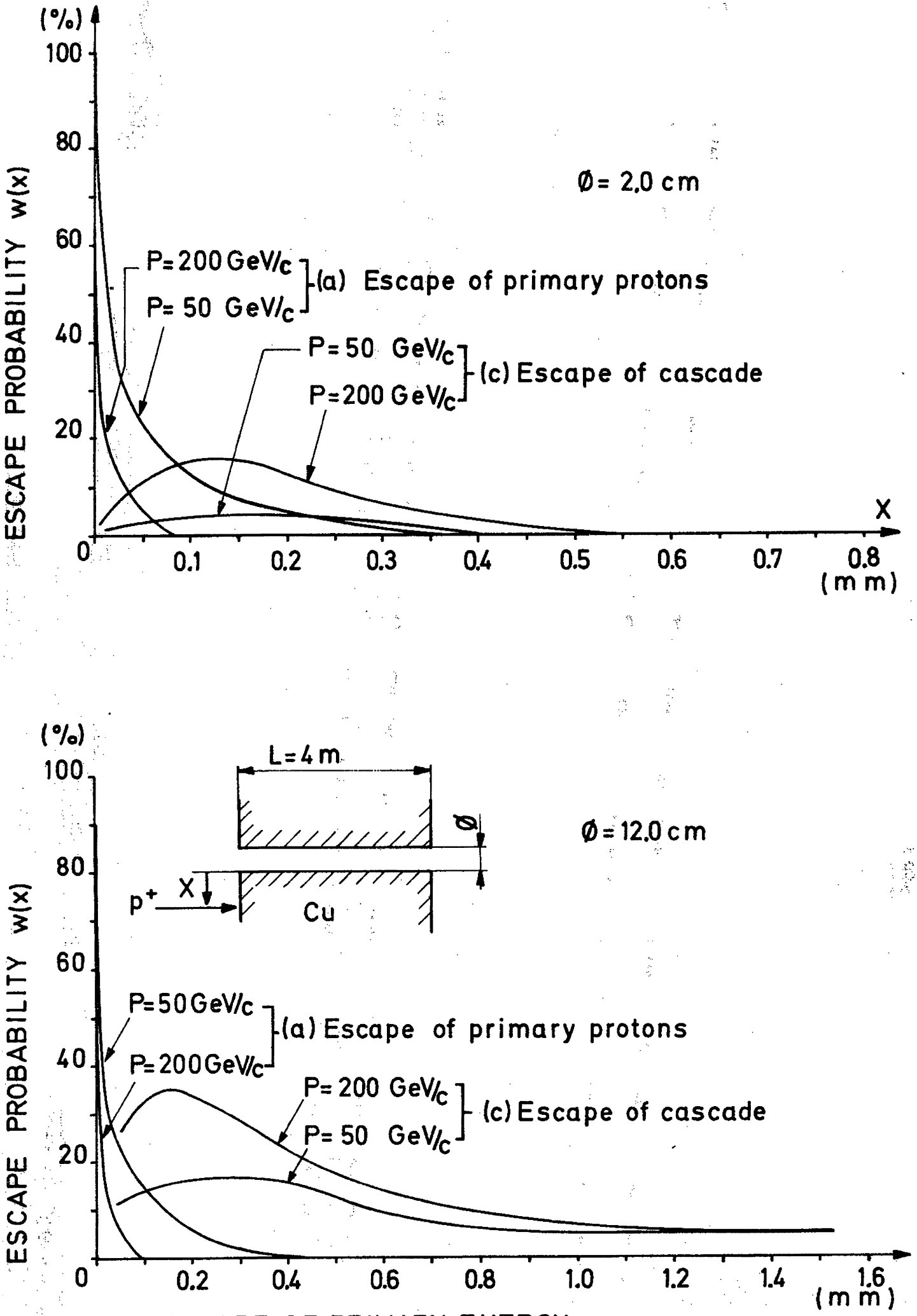

Fig. 5.2 ESCAPE OF PRIMARY ENERGY

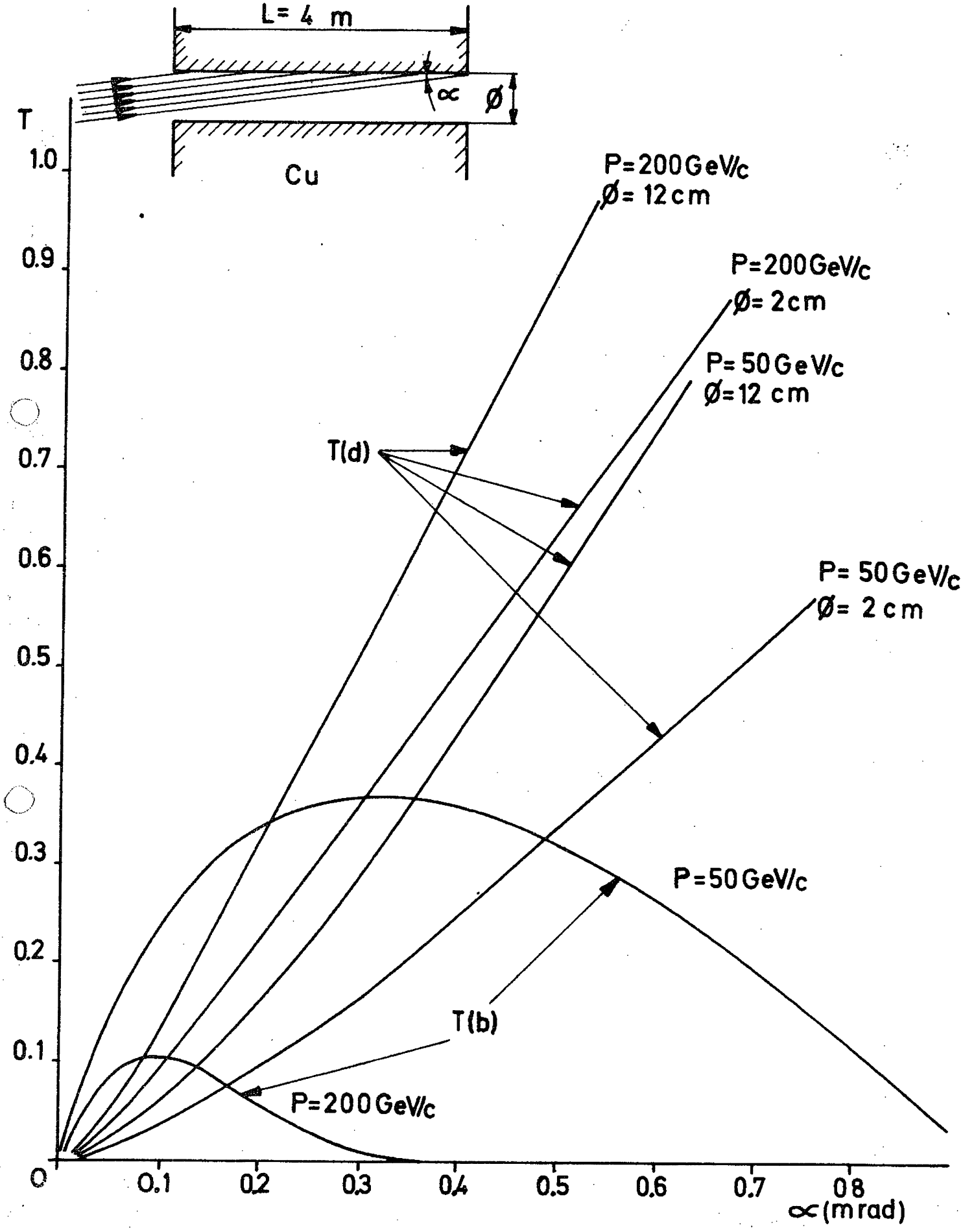

Fig 5.3 ESCAPE OF PRIMARY ENERGY

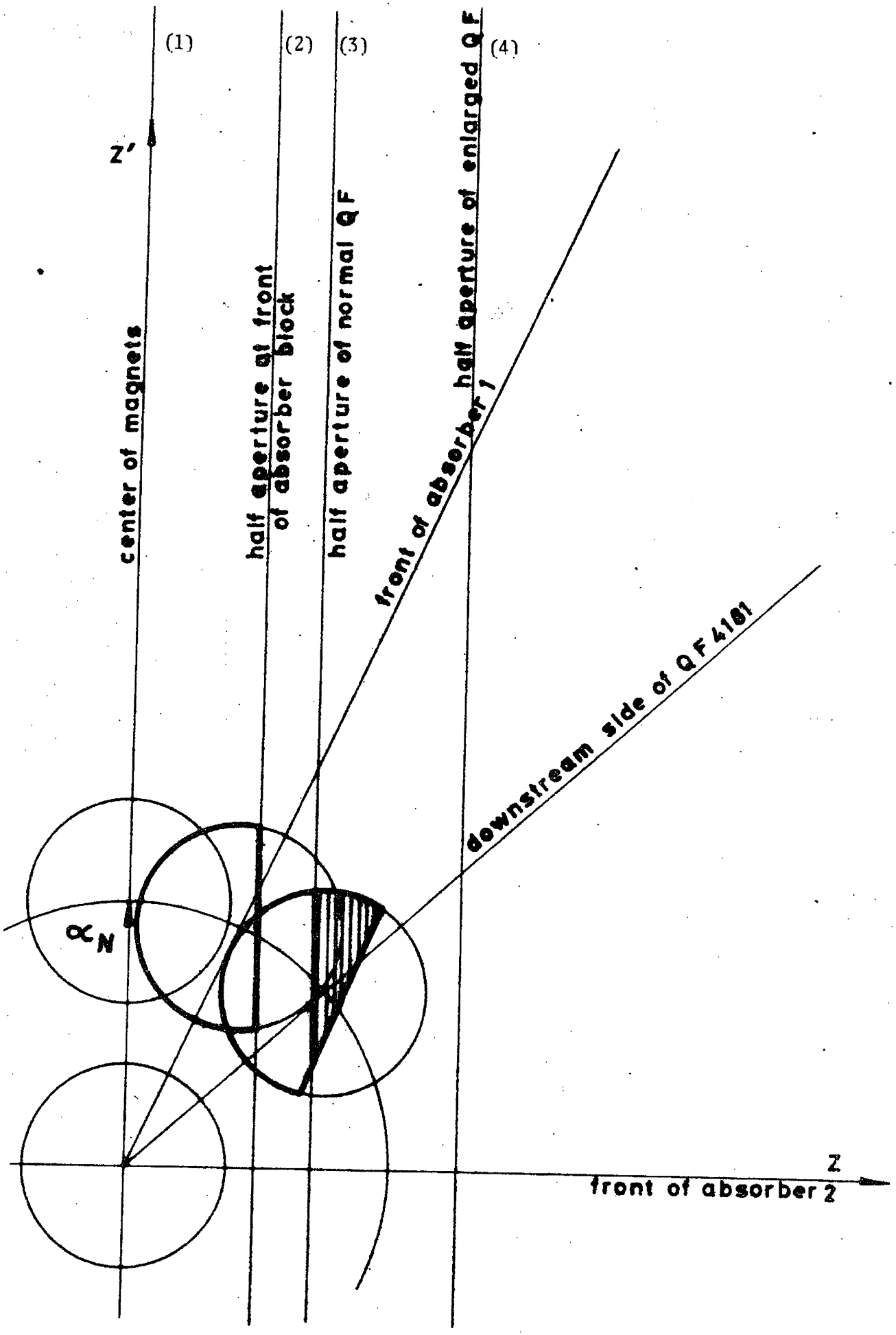

Fig III b1 Kicking in the normalized vertical phase plane with the nominal deflection angle

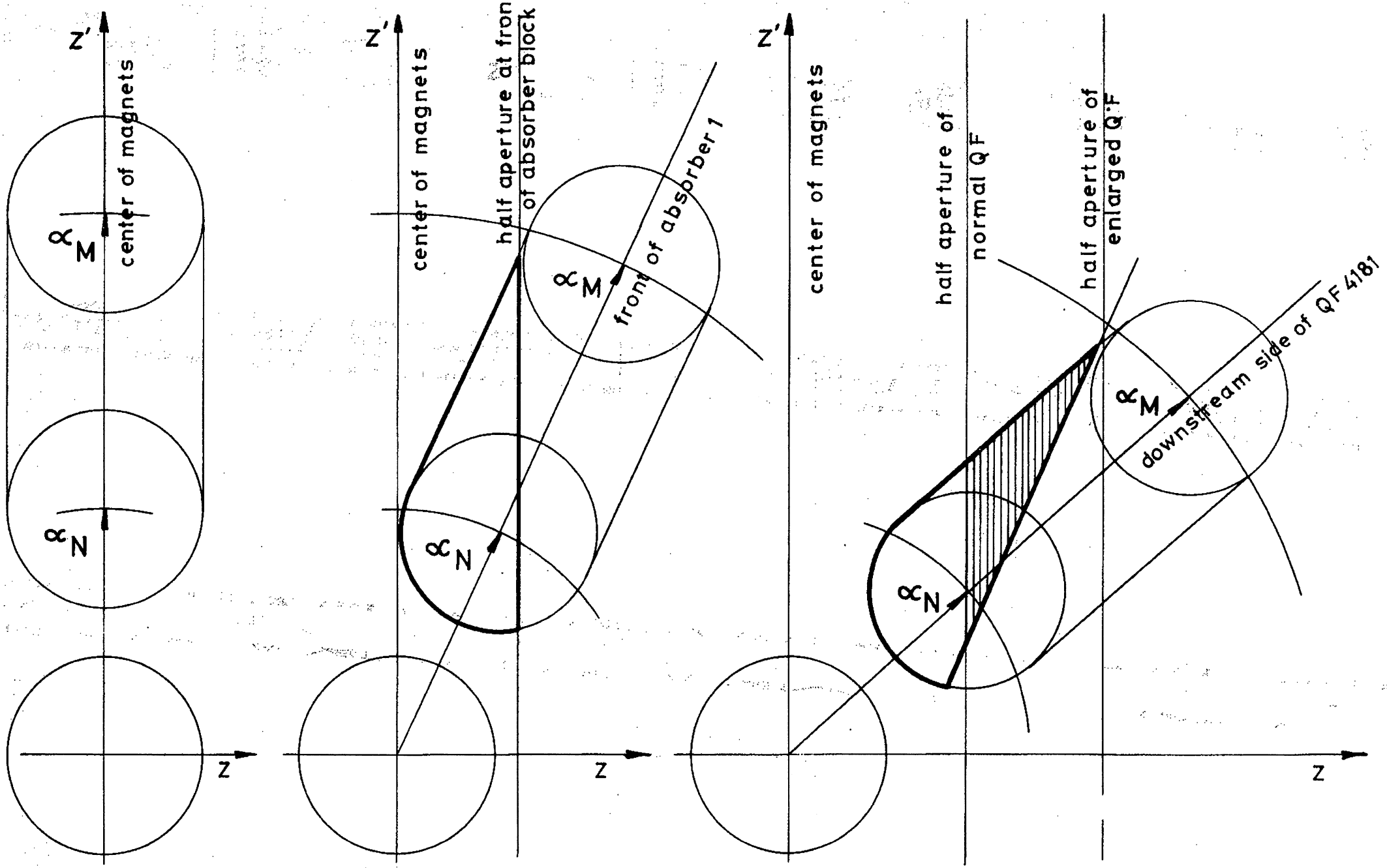

Fig III b 2 Kicking in the normalized vertical phase plane for a range of deflection angles between α_N and α_M (case of faulty voltage tracking)

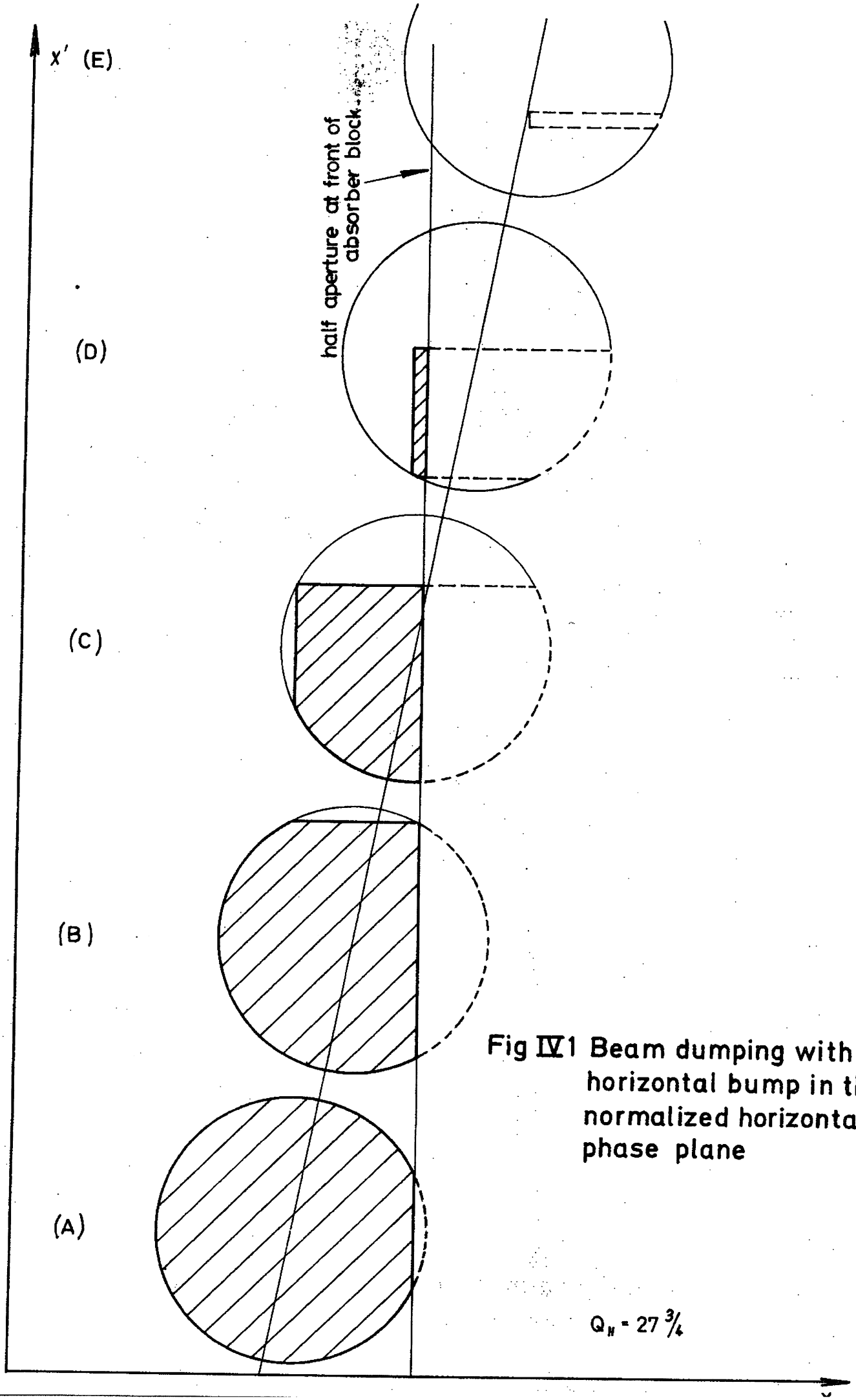

Fig IV.1 Beam dumping with a horizontal bump in the normalized horizontal phase plane

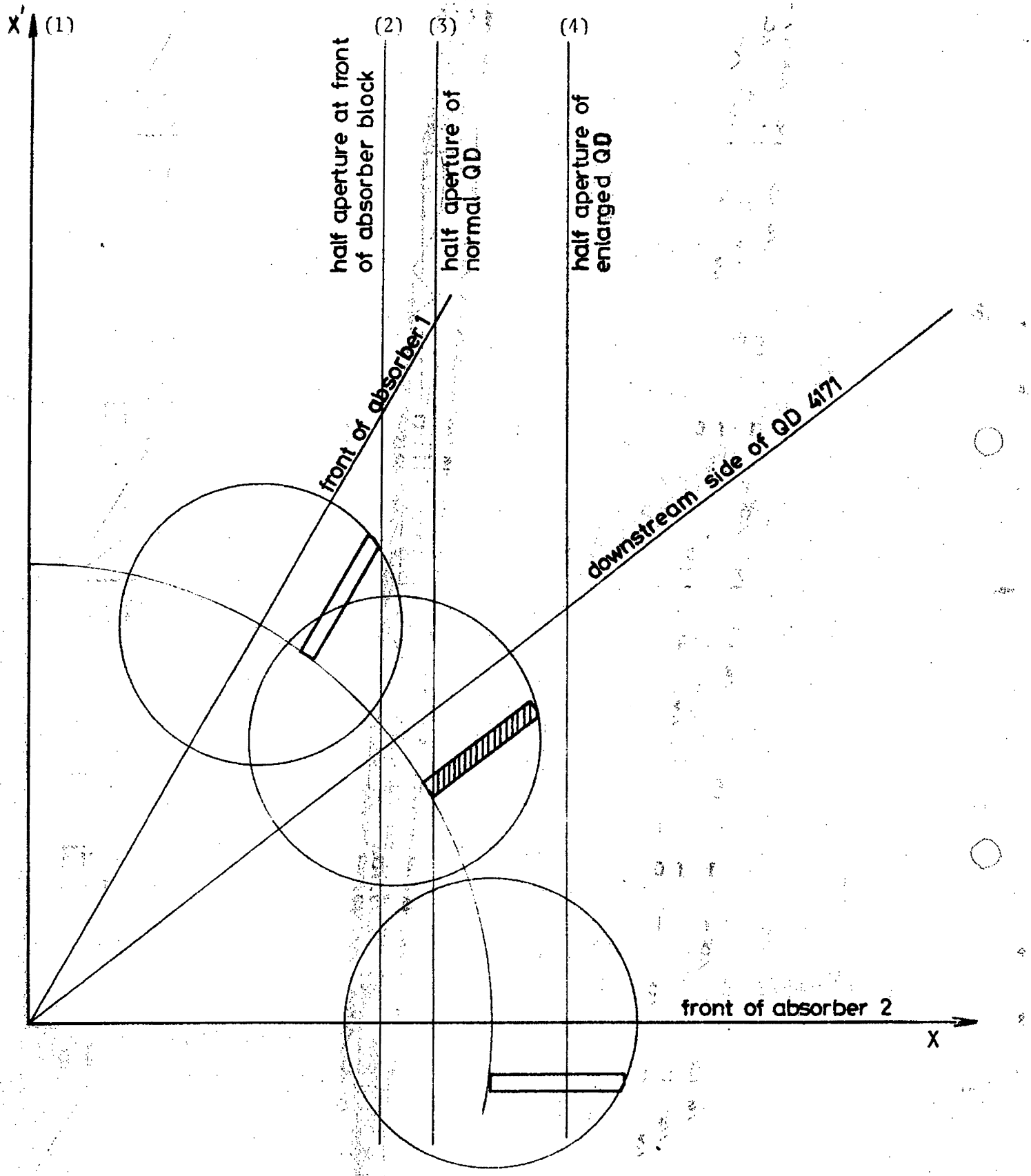

Fig IV 2 Beam dumping in the last revolution in the normalized horizontal phase plane